Journal of Biosciences and Medicines, 2026, 14(5), 360-392
https://www.scirp.org/journal/jbm
ISSN Online: 2327-509X
ISSN Print: 2327-5081

An Integrated Single-Cell Transcriptomic Atlas of Human Tricuspid and Aortic Valve Diseases

Jingyi Wang[1*], Mingke Wu[1*], Dingjie Xu[1], Rong Jin[1], Jie Hao[1], Xin Wang[2,3], Qing Ge[1,4,5#]

[1]NHC Key Laboratory of Medical Immunology (Peking University), Medicine Innovation Center for Fundamental Research on Major Immunology-Related Diseases, Department of Immunology, School of Basic Medical Sciences, Peking University, Beijing, China
[2]Department of Cardiac Surgery, Fuwai Hospital, National Center for Cardiovascular Diseases, Chinese Academy of Medical Sciences and Peking Union Medical College, Beijing, China
[3]State Key Laboratory of Cardiovascular Disease, Fuwai Hospital, National Center for Cardiovascular Diseases, Chinese Academy of Medical Sciences and Peking Union Medical College, Beijing, China
[4]Beijing Electric Power Hospital, Key Laboratory of Geriatrics (Hepatobiliary Diseases), China General Technology Group, Beijing, China
[5]Department of Integration of Chinese and Western Medicine, School of Basic Medical Sciences, Peking University, Beijing, China
Email: [#]qingge@bjmu.edu.cn

How to cite this paper: Wang, J.Y., Wu, M.K., Xu, D.J., Jin, R., Hao, J., Wang, X. and Ge, Q. (2026) An Integrated Single-Cell Transcriptomic Atlas of Human Tricuspid and Aortic Valve Diseases. *Journal of Biosciences and Medicines*, **14**, 360-392.
https://doi.org/10.4236/jbm.2026.145025

Received: April 15, 2026
Accepted: May 23, 2026
Published: May 26, 2026

Abstract

Tricuspid regurgitation (TR) and calcific aortic valve disease (CAVD) are two common valvular heart diseases with distinct pathological characteristics. However, a systematic single-cell level comparison of their cellular composition and transcriptional profiles remains limited. In this study, we analyzed publicly available single-cell RNA sequencing (scRNA-seq) datasets from human tricuspid valve (TV) and aortic valve (AV) tissues, including samples from TR and CAVD patients as well as corresponding control samples. A total of 128,817 cells passed quality control (QC) from an initial 138,568 cells across all samples. We constructed a processed single-cell dataset covering major valvular cell populations, including valvular interstitial cells (VICs), valvular endothelial cells (VECs), and immune cell populations. Cell type annotation, gene expression profiles, and basic transcriptional differences across disease and control groups were described. In addition, we summarized differences in inferred cell-cell communication patterns between TR and control TV samples and provided a comparative description between TR and CAVD datasets. The processed expression matrices, cell annotations, and metadata have been deposited in the Zenodo repository and are publicly available for reuse. This study provides a single-cell transcriptomic dataset resource for further exploration of human valvular diseases.

*Co-first authors.
[#]Corresponding author.

Keywords

Single-Cell RNA Sequencing, Tricuspid Regurgitation, Calcific Aortic Valve Disease, Valvular Interstitial Cells, Valvular Endothelial Cells

1. Introduction

Tricuspid regurgitation (TR) is a prevalent valvular heart disease, affecting 65% - 85% of the general population, with its incidence rising with age [1]-[3]. One of the prominent subtypes of TR is ventricular secondary TR, marked by right ventricle (RV) remodeling in response to increased pressure and/or volume overload [3] [4]. This remodeling process leads to the apical displacement of papillary muscles and the tethering of valve leaflets, which in turn causes significant TR and volume overload. This further exacerbates RV dimensions and wall stress [5]. A variety of cellular and molecular changes are implicated in RV remodeling, including inflammation, mitochondrial damage, metabolic shifts, myocyte replacement and loss, immune cell infiltration, and myocardial fibrosis [6]-[9]. However, a comprehensive characterization of the cellular and transcriptional features associated with tricuspid valve remodeling remains limited.

Calcific aortic valve disease (CAVD) is the most common indication for heart valve surgery. It is characterized by significant fibrosis and mineralization in the aortic valve (AV) leaflets, together with neovascularization and microhaemorrhage [10]. The differentiation of valvular interstitial cells (VICs) and valvular endothelial cells (VECs) into fibrocalcific lineages, driven by signaling pathways such as NOTCH, WNT, and myocardin, as well as complex interactions between these cells and immune cells, drives the remodeling of aortic valve leaflets and the progression of CAVD [10] [11].

The distinct ways in which VICs and VECs in the TV and AV leaflets respond to environmental cues during pathological remodeling are not well understood. Compared to the AV, the TV is an atrioventricular valve with a unique cellular composition. It contains lower percentages of mast cells and myofibroblasts, and higher percentages of specific VIC subsets, protective VEC subsets, and migratory anti-inflammatory T cell subsets [12]. Whether these differences contribute to the TV's relatively higher resistance to calcification and inflammatory diseases requires a direct comparison of cells in the TV and CAVD.

To this end, we integrated publicly available single-cell RNA sequencing (scRNA-seq) datasets of TVs from five patients with ventricle secondary TR and five control patients without TR (accession code HRA010091), as well as datasets from four patients with CAVD and two control patients without CAVD (PRJNA562645) [13]. The processed single-cell RNA sequencing data, including expression matrices, cell annotations, and metadata, have been deposited in the Zenodo repository and are publicly available at https://doi.org/10.5281/zenodo.19568228. We systematically characterized the cellular composition, transcriptional programs, and in-

ferred intercellular communication patterns across resident and infiltrating cell populations in TVs and performed comparative analyses with CAVD datasets. This work provides a comprehensive resource for exploring cell-type-specific features and cross-disease differences in human valve biology.

2. Results

2.1. Enhanced VIC Activation, Oxidative Stress, and Myofibroblast Differentiation in TR-Derived Tricuspid Valve

To investigate the transcriptome features of TV that contribute to their higher resistance to calcification, we integrated the publicly available scRNA-seq datasets from TR (accession number HRA010091) and CAVD (PRJNA562645) [13]. A total of 128,817 cells passed quality control (QC) from an initial 138,568 cells across all samples. The detailed patient information and cell counts per sample before and after QC are provided in Supplementary Table. The R package "Harmony" was used to correct for batch effects. After rigorous processing of the raw data, which included the removal of low-quality cells and doublets, a total of 93,916 cells from TR and their TV controls, and 34,901 cells from CAVD and their AV controls, were integrated and clustered (**Figures 1(A)-(C)**). Seven major cell types were identified using cluster-specific biomarkers, VICs, myofibroblasts, VECs, mast cells, myeloid cells, T/NK cells, and a distinct population of valve-derived stromal cells (VDSCs) [14] in CAVD/AV but not in TR/TV samples (**Figures 1(A)-(C)**). The VDSC cluster was identified by the expression of inflammatory and mesenchymal activation markers (*INHBA*, *CXCL*1, *CCL*20, *ID*4, *SOX*4) [15]. Myofibroblasts were identified by the expression of *TAGLN*, *ACTA*2, *ITGB*1, and *THBS*2 [16]. The nerve-like VIC population was supported by an enrichment of ECM and neuro-associated genes (*VCAN*, *TTYH*1, *LGI*4, *VEGFA*) [16]. The VICs and VECs in both CAVD/AV and TR/TV groups were less aggregated than the immune cells (T/NK and myeloid cells) (**Figure 1(A)**).

Given that the cell atlas of tricuspid valves is less well studied compared to that of aortic valves, we first focused our analysis on various cell types in TR and control TV samples. The TR/TV-derived VICs and myofibroblasts were subclustered, and seven distinct VIC clusters were identified, each with unique gene expression profiles and transcriptional regulons (**Figure 1(D)**, **Figure 1(E)**, **Figure S1(A)**, **Figure S1(B)**). The F5 cluster was characterized as resident VICs due to high expression of *TCF*21, *CD*34, *OSR*1, and the active transcription factor OSR1, which promotes myogenesis (**Figure 1(E)** and **Figure S1(B)**) [17] [18]. The F1 cluster exhibited high expression and activity of GATA4, potentially involved in myocardial capillarization under pressure overload (**Figure 1(E)** and **Figure S1(B)**) [19]. Clusters F2 and F3 were annotated as inflammatory VICs due to their expression of chemokines (CCL2 and CXCL12) and type I interferon (IFN)-regulated genes (**Figure 1(E)**). The F4 cluster was identified as a structural VIC cluster, enriched in transcriptional regulons related to fibroblast activation and

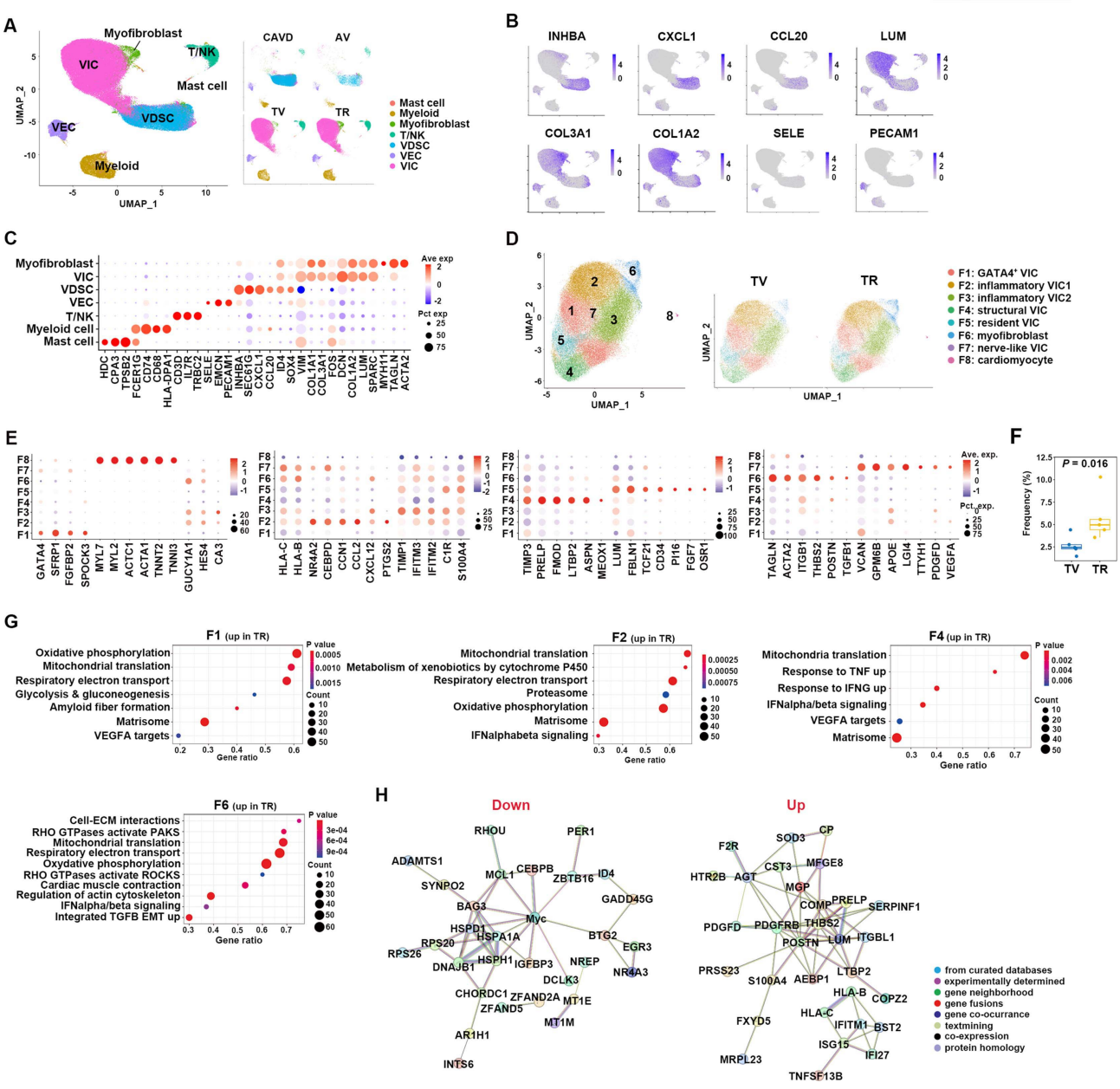

Figure 1. Cell composition of tricuspid and aortic valve leaflets (A)-(C) and comparison of the transcriptome features of VICs between TV and TR groups (D)-(H).

pathological cardiac fibrosis (MEOX1 and KDM5B) [20] [21], and expressed genes involved in ECM production, remodeling, and degradation (**Figure 1(E)** and **Figure S1(B)**). The F6 cluster was characterized as a *POSTN*$^{+}$ myofibroblast cluster with features of healing and scar formation [22], while F7 was designated as a nerve-like VIC cluster based on specific gene expression patterns (*LGI4* [23], *GPM6B* [24], *TTYH1* [25] and enriched transcriptional regulons (TEAD [26], SOX9, TBX20, IRF7 [27]-[29]) (**Figure 1(E)** and **Figure S1(B)**). Previous studies have identified *GUCY1A1*- and *HES4*-expressing NO-associated VIC clusters in adult heart-derived non-diseased TVs and an *APOE*$^{+}$ elastin-VIC cluster in fetal

heart-derived valves [12] [30]. A few cardiomyocytes with high expression of genes encoding myosin light chains and troponin were also identified, designated as the F8 cluster (**Figure 1(D)**, **Figure 1(E)**). In our dataset, cells expressing these markers were enriched in inflammatory VICs (F2 and F3), myofibroblasts (F6), and nerve-like VICs (F7) (**Figure 1(E)**). However, elastogenesis-related genes such as *ELN* and *EMILIN*1 were not found in any VIC clusters. Notably, these VIC clusters expressed high levels of MHC class I and IFN-regulated genes, suggesting a potential role in antigen presentation to $CD8^+$ T cells.

We next compared the VICs between the TR and control TV groups. At the cellular level, the myofibroblast (F6) cluster was significantly more prevalent in the TR group (**Figure 1(F)** and **Figure S1(C)**).

At the transcriptome level, VICs in the TR group exhibited increased expression of genes associated with cell metabolism, IFNα/β signaling, and the matrisome compared to the Ctrl group (**Figure 1(G)** and **Figures S1(D)-(F)**). Structural VICs (F4) in the TR group further up-regulated VEGFA targets and their responsiveness to TNF-α and IFN-γ, while myofibroblasts (F6) up-regulated genes involved in endothelial-mesenchymal transition (EMT) and cardiac muscle contraction (**Figure 1(G)**). Notably, VICs in the TR group revealed significant down-regulation of the elastogenesis regulator *APOE*, proteostasis-regulator heat shock proteins (HSPs), and oxidative-stress inhibitor metallothioneins (MTs) (**Figure S1(E)**, **Figure S1(F)**) [30]-[33]. STRING analysis of these DEGs revealed that the up-regulated genes were associated with the network of ECM and IFN responsiveness (*BST*2, *IFITM*1, *ISG*15, *IFI*27, and HLAs), while down-regulated genes were involved in protein stability and negative regulation of cellular metabolic process (**Figure 1(H)**). Pseudo-time analysis indicated that the TR group had defects in the upregulation of growth factor *MDK* (midkine) [34] and the cardioprotective molecule *NCL* (nucleolin) [35], and down-regulation of the EMT-promoting molecule *POSTN* (periostin) [36] along the cell differentiation path (**Figure S1(G)**). Collectively, these results indicate that the TR samples exhibit elevated VIC activation and fibrosis, characterized by upregulation of IFN responsiveness, ECM production, and oxidative stress, enhanced myofibroblast differentiation, and impaired proteostasis.

2.2. Altered Cellular Interaction within VIC Clusters and between VICs and Other Cell Types in TR-Derived Tricuspid Valve

In the tricuspid valves, VICs accounted for the majority of interactions among all cell types (**Figure 2(A)**). Compared to the control TV group, the TR group exhibited a marked reduction in cellular communication both among various cell types and within VICs themselves (**Figure 2(B)**). The most significantly down-regulated ligand-receptor pairs in the TR group were cardioprotective heparin-binding growth factors and their glycosylated protein receptors [37]-[40] (MDK-SDC2, MDK-NCL, PTN-SDC2, PTN-NCL), which are involved in interactions within VICs, between VICs and myofibroblasts, and between VICs and T/NK

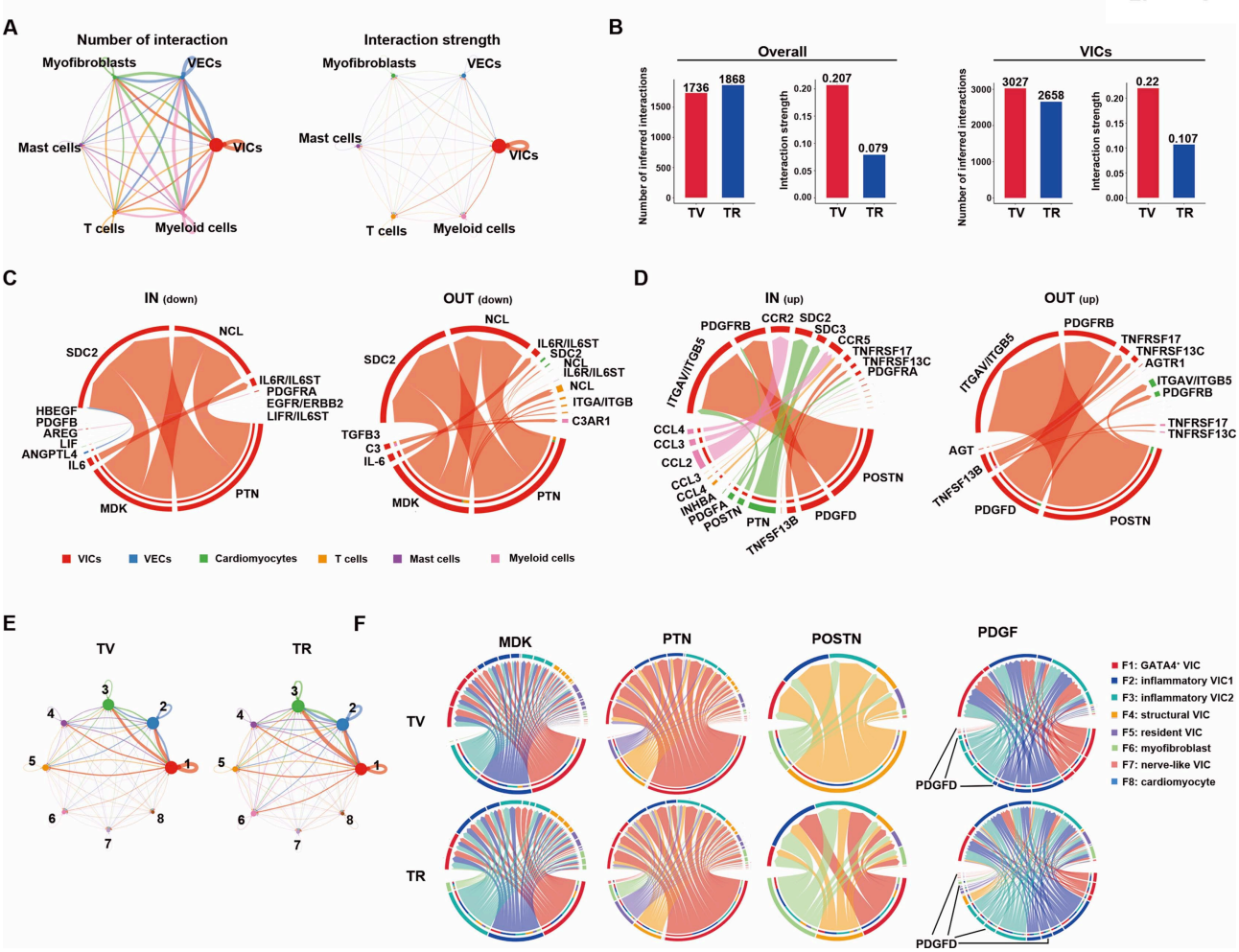

Figure 2. General characteristics and comparison of the inferred intercellular ligand-receptor interactions between TV and TR groups.

cells (Figure 2(C)). Additionally, interactions involving the pro-inflammatory cytokine IL-6 and its receptor within VICs, as well as the anti-inflammatory molecule ANGPTL4 [41] [42] in VECs and its binding partner HBEGF in VICs, were also decreased in the TR group (Figure 2(C)). Conversely, the TR group showed an upregulation of profibrogenic factors [43]-[45] and their receptors, such as POSTN-ITGAV/ITGB5 and PDGFD-PDGFRB, both within VICs and between VICs and myofibroblasts (Figure 2(D)). Communication between immune cells and VICs, mediated by inflammatory chemokines (CCL2, CCL3, and CCL4) and their receptors, was also heightened in the TR group (Figure 2(D)).

Further analysis of the crosstalk within VIC clusters revealed dominant communication between GATA4$^+$ (F1) and two inflammatory VIC clusters (F2 and F3), with the TR group exhibiting increased interaction strength compared to the control TV group (Figure 2(E)). Enhanced communication between these VIC clusters and myofibroblasts (F6) was also observed in TR samples (Figure 2(E)). The patterns of cellular communication involving MDK, PTN, POSTN, and PDGFD and their respective receptors differed between the TR and control TV

groups (**Figure 2(F)**). In the TV group, MDK produced by GATA4$^+$ and inflammatory VICs primarily regulated themselves, while GATA4$^+$, structural, and resident VICs sent pro-angiogenic factor PTN to GATA4$^+$ and inflammatory VICs (**Figure 2(F)**). In the TR group, this interaction pattern was attenuated, with a substantial increase in communication between inflammatory VICs/myofibroblasts and other VIC clusters (**Figure 2(F)**). The primary sources of POSTN also shifted from the structural VIC cluster (F4) in the control TV group to GATA4$^+$ VIC and myofibroblasts in the TR group (**Figure 2(F)**). Together, these results indicate that TVs in TR patients are associated with significantly altered cellular communication, characterized by a reduction in cardioprotective signaling but an enhancement in profibrogenic crosstalk within VIC clusters and between VICs and other cell types.

2.3. Dysregulated VECs and Intercellular Communication with Pro-Inflammatory and Oxidative Stress Signature in TR-Derived Tricuspid Valves

VECs lining the TV serve as the initial cellular responders to shear stress and pressure fluctuations. Our analysis identified five distinct clusters among TR/TV-derived VECs (**Figures 3(A)-(C)** and **Figure S2(A)**, **Figure S2(B)**). The predominant cluster, referred to as protective VEC (E1), exhibited high expression levels of *COLEC*11 [12], *ENG*, *HLA*, as well as significant activity of transcription factors FOXC2 [46] and NFATC3 [47] [48] (**Figure 3(C)**). Although not statistically significant, a slight reduction in this cluster was observed in the TR group (**Figure S2(C)**). Compared to protective VECs (E1) from control TV samples, those from TR samples showed signs of oxidative stress, with upregulation of genes related to oxidative phosphorylation and reactive oxygen species, and downregulation of genes involved in TNF signaling through NF-κB (**Figure 3(D)**). Cluster E4 was characterized as repairing VECs due to their high expression of *WNT*, *NOS*3, *TAGLN*2, *ANGPTL*2, integrins, membrane transportation molecules, and repair molecules *S*100*A*10 and *S*100*A*11 [49], along with high activity levels of EMT-associated transcription factors (SNAI2 (Slug) and TEAD4) (**Figure 3(B)**, **Figure 3(C)**). However, the reparative function of these cells in the TR group appears to be compromised, as they exhibited upregulation of genes associated with TGFβ signaling and downregulation of genes related to NF-κB, hypoxia, EMT, apoptosis, and cell metabolism (**Figure 3(D)**). Cluster E5 was designated as shear stress-reactive VECs due to their expression of mechanosensitive channel *PIEZO*1, pro-angiogenic factor *SOX*17 [50], and von Willebrand factors (**Figure 3(B)**). High levels of transcription factor activity, including MEOX1, NFKB2, SMAD1, TEAD2, were also observed in E5 (**Figure 3(C)**). E5 cells from TR samples displayed a pro-inflammatory phenotype, with increased NF-κB signaling and inflammatory response, but reduced pro-angiogenic HEDGEHOG signaling and EMT (**Figure 3(D)**). The expression of flow-responsive genes, such as *KLF*4, *ADAMTS* [51], was also up-regulated in TR-derived E5 cells (**Figure 3(E)**). Notably, almost all VECs in TR samples showed an upregulation of the long non-coding

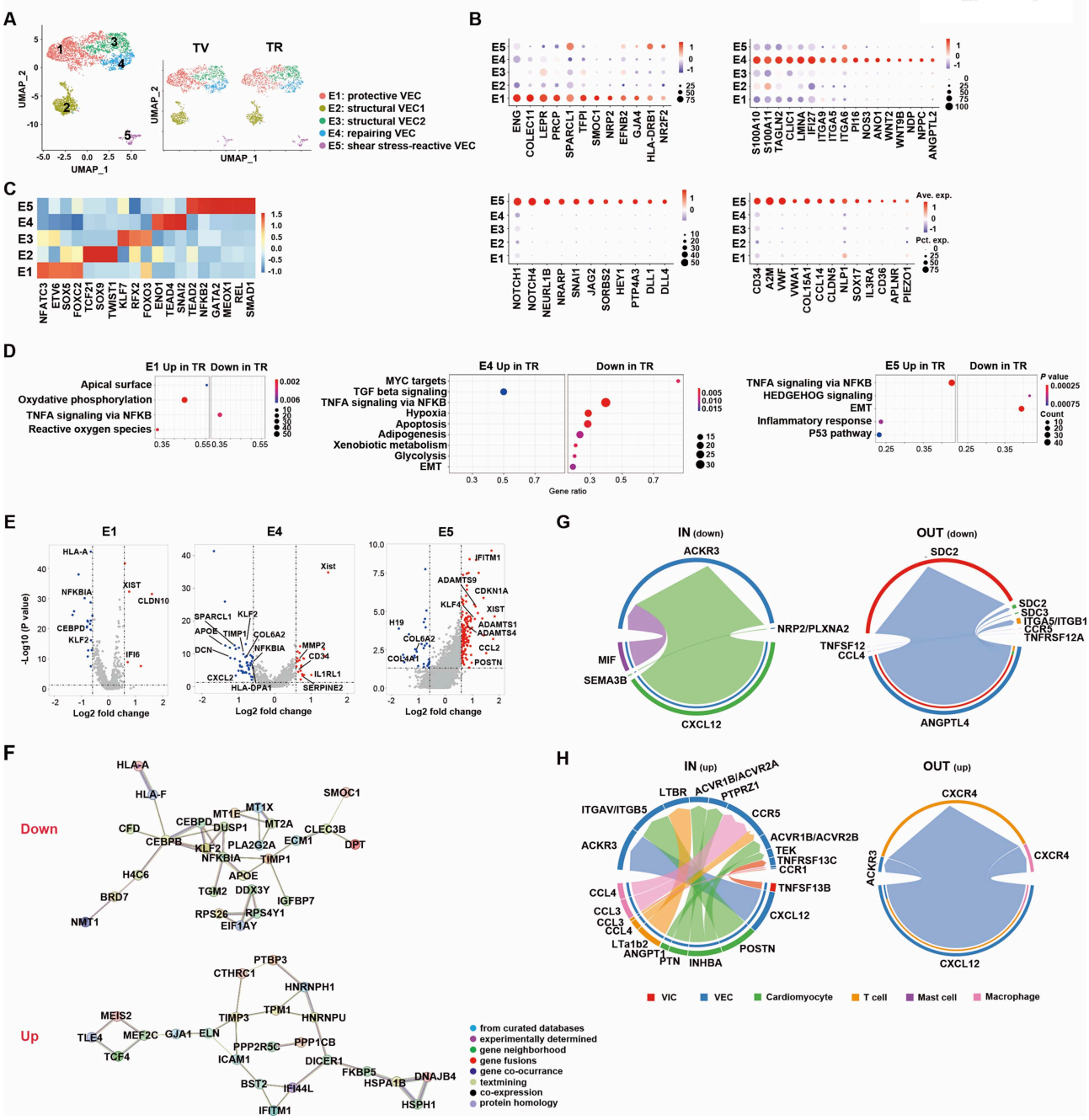

Figure 3. Comparison of the transcriptome features and intercellular interactions of VECs between TV and TR groups.

RNA *XIST* (X-inactive specific transcript), whose dysregulation has been implicated in cardiovascular diseases like fibrosis and hypertrophy [48] (**Figure 3(E)**, **Figure S2(D)**). STRING analysis of these DEGs revealed that up-regulated genes were associated with type I IFN and TGF-β responsiveness (*PTBP*3, *CTHRC*1, *TIMP*3) and negative regulation of cell proliferation, while down-regulated genes were linked to metallothioneins and collagen-containing ECM components (*TGM*2, *APOE*, *TIMP*1, *ECM*1, *CLEC3B*, *SMOC*1, and *DPT*) (**Figure 3(F)**). These findings suggest that VECs in the TR group are dysregulated, acquiring phenotypes indica-

tive of inflammation and oxidative stress, likely due to shear-stress-induced reprogramming.

We also investigated the intercellular communication between VECs and other cell types. We discovered that the TR group downregulated the anti-fibrogenic and anti-inflammatory VEC-VIC interaction (ANGPTL4-SDC2) [52] [53] but up-regulated profibrogenic VEC-myofibroblast interactions (POSTN-ITGAV/ITGB5 and INHBA/SCVR1B [54]) (**Figure 3(G)**, **Figure 3(H)**). Of note, the ability of VECs to scavenge myofibroblast-produced chemokine CXCL12 via ACKR3 [55] was diminished (**Figure 3(G)**, while their secretion of CXCL12 to recruit T/NK cells via CXCR4 was increased (**Figure 3(H)**). Consistently, interaction between immune cells and VECs via CCL3/4 and CCR5 was also elevated (**Figure 3(H)**). These results indicate that VECs in the TR group engage with other cells in a pro-inflammatory and profibrogenic manner.

2.4. Activated Myeloid Cells with Elevated Pro-Inflammatory and Profibrogenic Communication with VICs and Lymphocytes in TR-Derived Tricuspid Valves

Macrophages, both resident and monocyte-derived, play a crucial role in the regulation of cardiac remodeling. Our analysis identified nine macrophage clusters and one neutrophil cluster (*CSF3R*$^{+}$*S100A8*$^{+}$) based on gene expression profiles and transcriptional regulons (**Figures 4(A)-(C)**, **Figures S3(A)-(D)**). Four of these clusters (M1, M3, M4, and M5), which constituted 57.91% ± 10.25% of the total macrophages, expressed markers indicative of resident macrophage (RM), such as *CD*163 and *LYVE*1, along with the transcriptional regulon (MAFB and MAF) (**Figure 4(B)**, **Figure 4(C)**, **Figure S3(D)**) [56]-[61]. Among the *CD*163^{-} macrophages, we identified two MHC-II^{hi} clusters (M6 and M7) with high levels of pro-angiogenic cytokines *CXCL*16 and *IL*18 [62] [63], an *IL1B*-expressing pro-inflammatory cluster (M9), and a *DCN*-expressing myofibrolast-like macrophage cluster (M2) with high activity of transcription factors that promote valve remodeling and angiogenesis (TWIST1, GATA4, SOX9) [19] [28] [64]-[66] (**Figure 4(B)**, **Figure 4(C)**, **Figure S3(B)**). There were no significant differences in the abundance of these subpopulations between the TR and control TV groups (**Figure S3(E)**).

In comparison to the control TV samples, both CD163^{+} and CD163^{-} macrophages in TR samples were highly activated, as indicated by increased expression of genes related to cell metabolism, matrisome, initial complement triggering, antigen presentation, and chemokine/chemokine receptor interaction (**Figure 4(D)**). Notably, pro-inflammatory molecules such as *CCL2*, *CCL3*, *CCIA*, *S*100*A*8, and *S*100*A*9 were significantly up-regulated, while *VEGFA* and metallothionein genes were down-regulated in multiple TR-derived macrophage clusters (**Figure S3**F). Neutrophils, though sparse in the tricuspid valves, showed signs of activation in the TR group, with higher expression of matrisome- and oxidative phosphorylation-related genes (**Figures 4(A)-(D)**, **Figure S3(D)**). STRING analysis

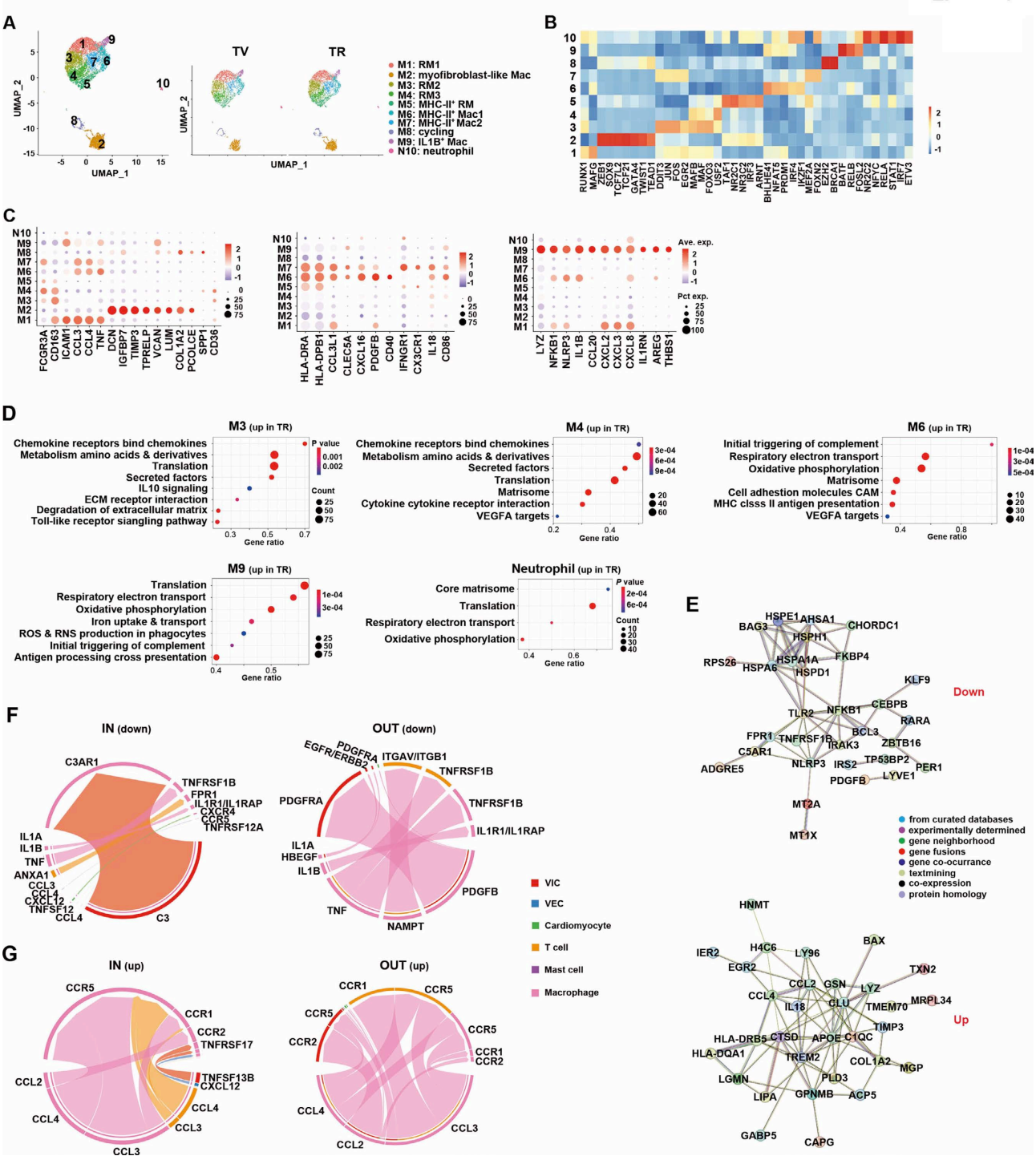

Figure 4. Comparison of the transcriptome features and intercellular communications of myeloid cells between TV and TR groups.

of these DEGs revealed that up-regulated genes were associated with the inflammatory response (*LY*96, *CCL*2, *CCL*4, *IL*18, *LGMN*, *BAX*, *CLU*, *TREM*2, *C*1*QC*, *HLA*), while down-regulated genes were linked to metallothioneins and positive regulation of IL-4 and IL-10 production (*HSPH*1, *HSPD*1, *TLR*2, *TNFRSF*1*B*, *NLRP*3, *BCL*2, *CEBPB*, *RARA*, *ZBTB*16) (Figure 4(E)). These data collectively

indicate that myeloid cells in TR exhibit high activation with pro-inflammatory and profibrogenic signatures.

We also observed close interactions between myeloid cells and T/NK cells, as well as between myeloid cells and VICs. Compared to the control TV samples, TR samples showed increased communication between myeloid cells and T/NK/VICs via chemokines CCL2, CCL3, CCL4, and their receptors (**Figure 4(F)**, **Figure 4(G)**). Conversely, interactions between these cells via C3-C3AR1, PDGFB-PDGFRA, TNF-TNFRSF1B, and NAMPT-integrin were decreased in the TR group (**Figure 4(F)**, **Figure 4(G)**). These data suggest that TR-derived myeloid cells are integral to the pro-inflammatory chemokine-chemokine receptor interaction pathway, being attracted and activated by these chemokines and further producing them to recruit more T/NK cells and influence VIC functions.

2.5. T/NK Cells with Enhanced Pro-Inflammatory Signature in TR-Derived Tricuspid Valves

The predominant lymphocyte populations in the tricuspid valves were *CREM*$^{+}$ CD4^{+} helper T (Th) cells and GZMB^{lo}*GZMA*^{hi} CD8^{+} T cells (**Figures 5(A)-(C)**). In comparison to the control TV group, T cells from the TR group exhibited minimal upregulation of genes, but there was a significant downregulation in the expression of multiple HSP genes, suggesting impaired proteostasis within the resident T cells (**Figure 5(D)**). Additionally, we identified an *FCGR3A*^{lo}*GZMA*$^{+}$ NK cluster that expressed high levels of chemokines *CCL4* and *XCL1*, as well as the reparative molecule *AREG*, but low levels of cytotoxicity-related molecules such as *GZMB* and *PRF1* (**Figure 5(A)**, **Figure 5(B)**). Notably, these NK cells in the TR group showed increased expression of pro-inflammatory molecules *CCL3*, *CCL4*, and *IFITM2*, and decreased expression of the reparative molecule *AREG* compared to those in the control TV group (**Figure 5(D)**).

We observed a decrease in VIC-T/NK communication via the MDK/PTN-NCL/integrin pathway and in T/NK-myeloid cell crosstalk via the anti-inflammatory ANXA1/FPR1 [67] axis in the TR group (**Figure 5(E)**). Conversely, TR samples demonstrated increased two-way communication between T/NK cells and myeloid cells via the pro-inflammatory CCL3/4 and CCR5/CCR1 pairs (**Figure 5(F)**). T/NK cells also contributed higher levels of CCL4 to VICs in TR samples (**Figure 5(F)**). The ligand-receptor pair CXCL12 and CXCR4, which mediate communication between VECs and T cells, was up-regulated in TR samples (**Figure 5(F)**). These results indicate that in TR, chemokines such as CCL3 and CCL4 recruit and regulate T/NK cells and macrophages, contributing to a pro-inflammatory environment that affects the differentiation and function of VICs. This also highlights close communication between GZMA^{+} T/NK cells and activated macrophages within the context of tricuspid valves in the TR group.

2.6. Mast Cells with Enhanced Profibrotic Signature in TR-Derived Tricuspid Valves

Mast cells serve as sentinels in the heart, swiftly responding to metabolic and immune

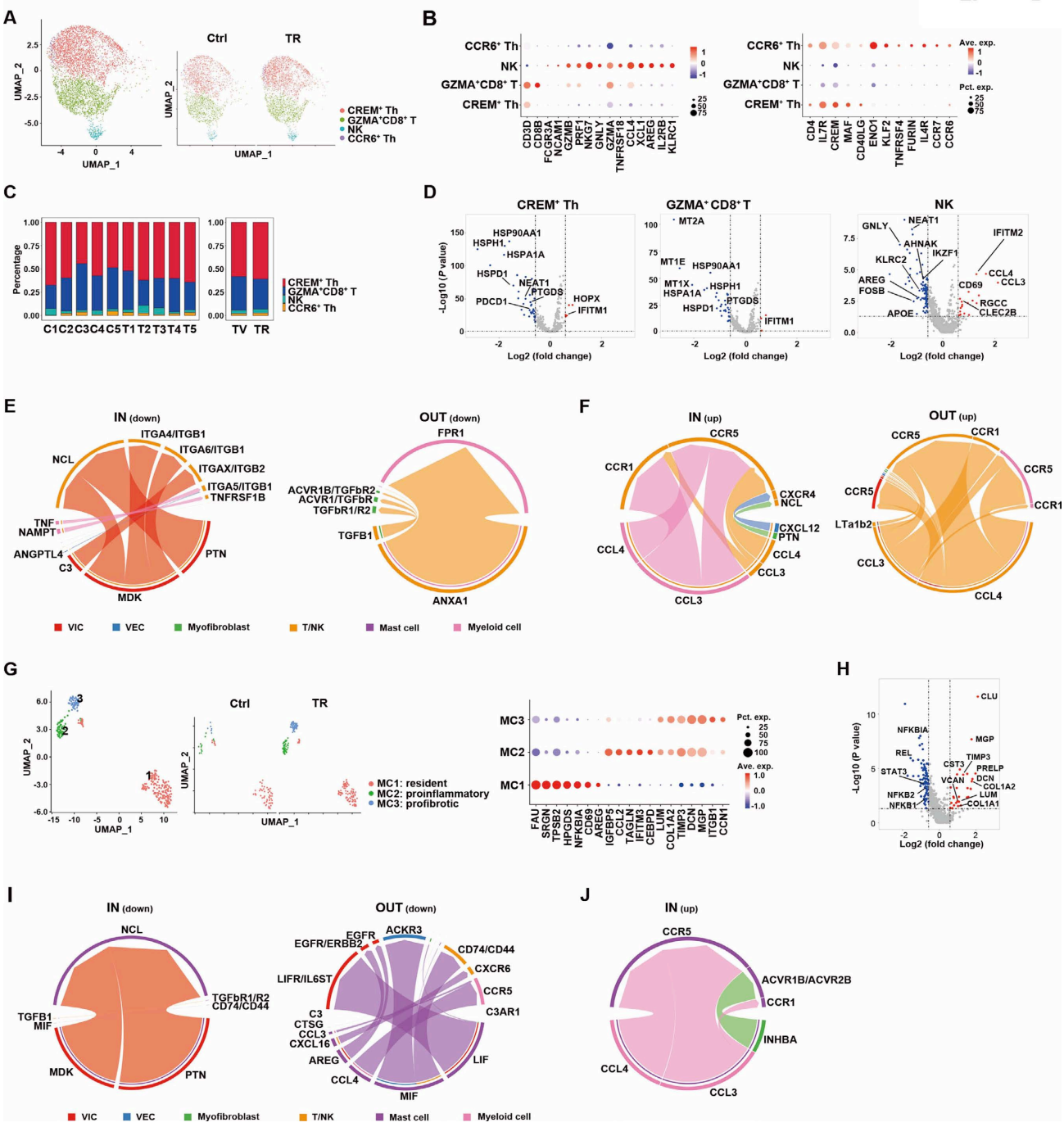

Figure 5. Comparison of the transcriptome features and cell interactions of T/NK and mast cells between TV and TR groups.

changes within their microenvironment. They have been reported to colocalize with macrophages, dendritic cells, and lymphocytes in stenotic human aortic valves [68]. In our study of tricuspid valves, we identified three distinct mast cell clusters, including *FAU*$^{+}$*CD69*$^{+}$ resident mast cells (M1), *CCL2*$^{+}$*IFITM3*$^{+}$ pro-inflammatory mast cells (M2), and *CCN1*$^{+}$*ITGB1*$^{+}$ profibrotic mast cells (M3) (**Figure 5(G)**). Given the small abundance of mast cells and the absence of significant differences in the distribution of mast cell clusters between the two groups, we

analyzed the transcriptome of these cells as a single population. Mast cells in the TR group exhibited significantly higher expression of fibrosis-associated genes and lower expression of NF-κB signaling genes compared to those in the control TV group (**Figure 5(H)**). We also observed that mast cells, which receive MDK and PTN from VICs and send various soluble factors to VICs, VECs, and immune cells, showed decreased activity in the TR samples (**Figure 5(I)**). Conversely, TR-derived mast cells received substantially increased levels of pro-inflammatory chemokines CCL3 and CCL4 from myeloid cells, and INHBA from myofibroblast (**Figure 5(J)**). These findings suggest that in TR, mast cells become dysregulated and adopt a profibrotic phenotype, likely due to the elevated levels of pro-inflammatory chemokines produced by activated myeloid cells.

2.7. TR-Derived Tricuspid Valves with Distinct Inflammatory Signature Compared to Calcific Aortic Valves

We next assessed the differences between TR and CAVD. Compared to VICs derived from TR, those derived from CAVD exhibited lower expression of genes related to ECM organization, TGFβ response, and cell-substrate adhesion, but higher expression of genes associated with myeloid leukocyte migration, ossification, oxidative stress response, and IL-1 cellular response (**Figure 6(A)**). Similarly, CAVD-derived VECs demonstrated significantly higher expression of genes involved in NF-κB signal transduction, TNF response, lipopolysaccharide (LPS) response, and myeloid leukocyte migration (**Figure 6(B)**). Notably, VICs and VECs from AV control samples exhibited up-regulated NF-κB signaling and responses to LPS and TNF compared to TV controls (**Figures S4(A)-(E)**). As shown in **Figure S4**, the unique cluster of VDSC in aortic valves also showed increased expression of genes associated with these pathways (**Figures S4(C)-(E)**). Immune cells in CAVD further exhibited increased LPS response and migration compared to those in TR (**Figure 6(C)**, **Figure 6(D)**).

Upon comparing cellular communication between the CAVD and TR groups, we found that, similar to TR samples, CAVD samples exhibited decreased cross-talk strength compared to AV controls (**Figure S5(A)**). In contrast to TR samples, VDSCs, rather than VICs, accounted for the majority of interactions among all cell types in CAVD (**Figure S5(B)**). Compared to TR samples, CAVD samples displayed increased expression of the pro-inflammatory chemokine CCL2 in VECs and VDSCs and enhanced interaction via CCL2-CCR2 and NAMPT-integrin among all cell types, including VDSCs (**Figure 6(E)**, **Figure 6(F)**, **Figure S5(C)**). The interaction mediated by MIF and its receptor between myeloid cells and other cells, such as VICs, VECs, T/NK cells, was also up-regulated (**Figure S5(D)**, **Figure S5(E)**). Conversely, downregulated communication in CAVD samples included anti-inflammatory pairs such as MDK, PTN, ANGPTL4, and their receptors within VICs, and between VECs and VICs (**Figure 6(E)**, **Figure 6(F)**). Additionally, interactions such as VEGFB-FLT1 between VICs and VECs, GZMA-F2R between T/NK and VECs or VICs, and CXCL12-CXCR4 between VICs and immune

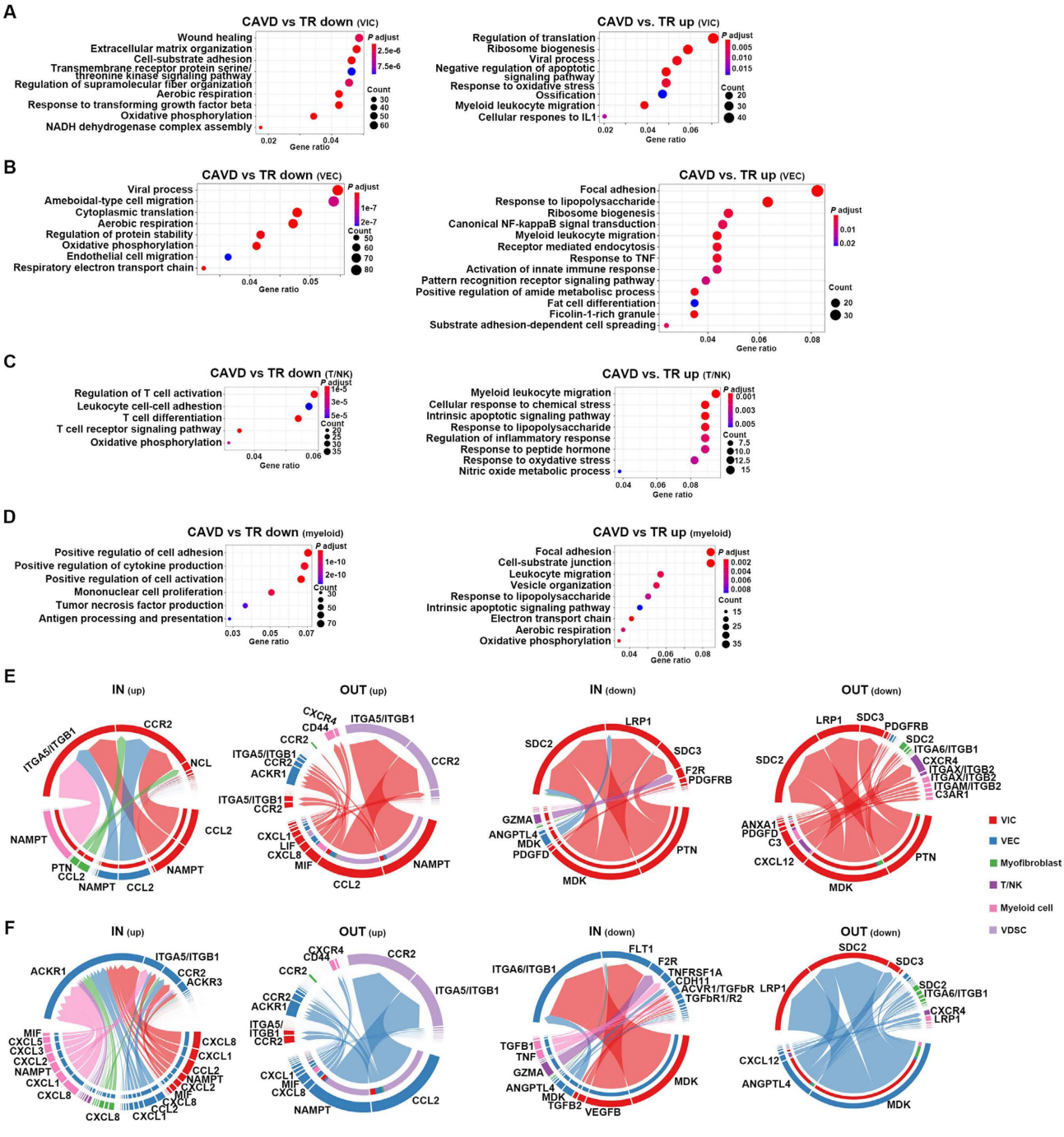

Figure 6. Comparison of the transcriptome features and intercellular communications between tricuspid valves obtained from TR and aortic valves obtained from CAVD.

cells were decreased (Figure 6(E), Figure 6(F), Figure S5(D), Figure S5(E)). These results collectively suggest that aortic valves, relative to tricuspid valves, are more susceptible to bacteria-induced inflammation, characterized by TNF response, NF-κB activation, and CCL2- and nicotinamide adenine dinucleotide (NAD^+)-mediated cellular communication. This highlights the distinct inflammatory signatures and cellular interactions between tricuspid valves and aortic

valves, which may underlie their differential resistance to calcification and inflammation.

3. Discussion

The TV is the largest yet thinnest valve in the heart [69] [70], and like other valves, it is continually exposed to high-pressure gradients and jet speeds within the circulation. The morphology of the leaflets, the anisotropic mechanical stress they undergo, the mechanobiology of the primary responding cell types—VECs and VICs—as well as immune cell activity, all potentially contribute to the relatively understudied valvular remodeling that occurs in the TV during the progression of TR [71]. In this study, we established a high-resolution transcriptomic landscape of TVs in TR patients, revealing that enhanced activation and oxidative stress in VICs and macrophages, increased pro-inflammatory communication and inflammatory responses among VICs, VECs, and immune cells, and elevated fibrogenesis are the main signatures in TR-TVs (**Figure 6(F)**). These factors likely contribute to the thickening of the TV leaflets and may promote a pro-inflammatory and profibrotic microenvironment, thus contributing to the pathogenesis of TR.

The constant and intricate interactions among VICs, VECs, macrophages, and lymphocytes are crucial for maintaining cardiac homeostasis, coordinating reparative responses to injury, and facilitating remodeling. In TVs, one significant communication pathway that was notably reduced in the TR group was mediated by heparin-binding growth factors MDK/PTN and their binding partners within VICs, from VICs to T/NK, and from VICs to mast cells. A paracrine mode of MDK has also been identified within VIC clusters in calcified aortic valves and between valve tissue and nearby cardiomyocytes, including those in the atrium [72] [73]. These ligand-receptor pairs have been implicated in the suppression of aortic VIC calcification and in promoting angiogenesis and tissue regeneration [72].

Our results further revealed that T/NK and mast cells are also the recipients of MDK signals. While MDK is known to promote immune cell chemotaxis and inhibit anti-tumor responses of T cells in tumor models [74], its impact on mast cell function is less clear. However, given that MDK is generally protective to the heart in cases of ischemic injury, it is probable that MDK-mediated cellular communication may suppress the activation of lymphocytes and VICs and promote cellular homeostasis in TV. Other anti-inflammatory interactions in TV include atypical chemokine receptor ACKR3, expressed on VECs to scavenge CXCL12 produced by myofibroblasts and MIF by mast cells. This communication regulates the bioavailability of these cytokines and may also contribute to angiogenesis and resistance to oxidative stress in endothelial cells [75]-[78], as the deletion of ACKR3 in mice resulted in increased VIC proliferation, TGFβ/BMP signaling, and aortic and pulmonary valve thickening and stenosis [79].

The up-regulated cellular interaction in TR-derived TVs was primarily mediated by chemokines CCL3/4, produced by macrophages and T/NK cells, and their

receptor CCR5, expressed on immune cells, VICs, VECs, and mast cells. CCR5 expression has been found in human sclerotic valve, and the polymorphism of CCR5 (CCR5 del32) is associated with a higher degree of calcification of stenotic aortic valves [80] [81]. The contributions of CCR5 to aortic stenosis with pressure overload-induced left ventricle remodeling, atherosclerosis, Ang II-induced hypertension, and vascular dysfunction [82]-[84] have also been reported, suggesting a similar pro-inflammatory and profibrotic role of CCR5 in TV remodeling. Therefore, the dysregulation of anti-inflammatory and pro-inflammatory interactions within TR-TVs likely facilitates the activation of myeloid cells and VICs, promoting fibrogenesis. Targeting CCR5 may help delay the fibrosis and thickening of TVs.

TV leaflets are unique among cardiac valves, possessing distinct VIC and VEC subsets compared to other cardiac valves [12]. Differences in VIC mechanical properties have also been reported, with VICs from the left side of the heart exhibiting higher stiffness and greater expression of αSMA and heat shock protein 47 [85] [86]. Our results provide transcriptome evidence that these cells in TVs and AVs respond to mechanical stress in significantly different ways. TGFβ- and TNF-α-NF-κB-induced endothelial-mesenchymal transition (EndMT) [87] and subsequent osteogenesis have been reported as major players in aortic valve calcification [88]. However, we found enhanced TGFβ signaling but decreased IL-1 response and TNF signaling via NF-κB in TR-VECs, and an absence of EndMT-driving differentiation of VDSCs from VICs and VECs [13] in TR compared to either non-diseased TV controls or CAVDs. Decreased interaction of TNF and its receptor was also observed within myeloid cells and between myeloid cells and T/NK cells. Additionally, bacteria have been found in aortic valves, and species such as *Corynebacterium matruchotti* and *Streptococcus sanguis* II contribute to recurrent low-grade endocarditis and aortic valve calcifications [89]-[91]. Inflammation induced by bacteria-derived LPS has been shown to stimulate osteogenic responses in AV-derived VICs [92]. In the context of TR, we observed lower levels of LPS response in VECs and immune cells, as well as reduced inflammatory cellular interactions via the CCL2-CCR2 axis. Since EndMT requires inflammatory factors beyond TGFβ, such as TNF and IL-1, to stabilize its progression and associated pathology [93], this raises the possibility that microbiota/inflammation-associated EndMT may be less extensive in TR-derived TVs than has been reported in CAVDs. This observation is consistent with the transcriptomic finding that TR-derived TVs exhibit more activated VIC signatures with enhanced wound healing capability and fewer ossification-associated transcripts relative to published CAVD data.

Our analysis of single-cell RNA sequencing data from tricuspid regurgitation-derived TVs allowed us to identify transcriptome signatures across various cell types and subpopulations, as well as intercellular communications. Our analyses identified dysregulated cellular communication among resident and infiltrating cell populations along with an inflammatory transcriptomic signature that ap-

pears distinct from previously reported patterns in CAVD, suggesting potential relevance to the pathogenesis of TR and offering possible insights into future strategies to delay the progression of tricuspid regurgitation.

Nevertheless, our findings did not elucidate the initial triggers and promoters of the unique inflammation and fibrosis observed in VECs and VICs of TVs. Additionally, the reasons for the lower response to LPS, reduced TNF and NF-κB signaling, decreased CCL2-CCR2 interaction, and minimal EndMT in VECs from TR-derived TVs compared to those from CAVD remain unclear. The specific contributions of gut microflora and its metabolites to the distinct inflammatory responses and subsequent fibrosis and/or calcification in aortic and tricuspid valves need more detailed investigation. Further studies are required to characterize the effects of various mechanical stresses, matrix composition, and stiffness, as well as cell-cell and cell-matrix interactions, in order to comprehend the mechanisms underlying the thickness of TV and the progression of TR.

4. Methods and Materials

4.1. Scrna-Seq Data Preprocessing and Quality Control

The scRNA-seq data in FASTQ files were processed by Cell Ranger software (Version 6.1.2, 10× genomics). The sequencing reads were demultiplexed, mapped to the GRCh38 human reference genome, and counted by unique molecular identifier (UMI). The UMI count matrix was then analyzed using the Seurat package (v4.4.0) in R software (v4.3.1). The cells expressing hemoglobin genes (*HBA*1, *HBA*2, *HBB*, *HBD*, *HBE*1, *HBG*1, *HBG*2, *HBM*, *HBQ*1, *HBZ*) were removed from the data set, as they likely represented erythrocytes. Only the cells with 200~6000 detected genes and <10% mitochondrial UMIs were considered valid cells and used for downstream analysis. After the quality control, there were 91,018 cells and 26,179 genes for downstream analysis.

4.2. Clustering and Cell Type Annotation

After normalizing and scaling, the "RunPCA" function in Seurat was used for Dimension reduction. The R package "Harmony" was used to remove batch effects. The "RunUMAP" function was performed to visualize each cell. The differentially expressed genes (DEGs) of the cluster were calculated by the "FindAllMarkers" function. Cell types were annotated based on differentially expressed genes (DEGs) of each subcluster.

4.3. Cell Cycle Analysis

The Seurat function CellCycleScoring was used to predict the cell cycle stage of each individual cell in a given cluster. Previously well-defined S and G2/M phase marker genes were used to calculate the S score and G2/M score, respectively.

4.4. DEGs Identification and Pathway Enrichment

The DEGs between Ctrl and TR groups were calculated by the "FindMarkers" function. Gene Set Enrichment Analysis (GSEA) was performed using the R pack-

age cluster-Profiler (Version 3.18.1) based on the hallmark gene sets or curated gene sets described in the MSigDB database. Gene Ontology (GO) Analysis was performed using the R package cluster-Profiler (Version 3.18.1) based on the DEGs. Statistical note: The "FindMarkers" function used a Wilcoxon rank-sum test at the single-cell level, treating each cell as an independent observation. This approach does not explicitly account for donor-to-donor biological variation, which may lead to inflated statistical significance.

4.5. Cell-Cell Ligand-Receptor Interaction Analysis

Cellchat (v1.6.1) was applied for ligand-receptor analysis. The raw counts and cell type annotation for each cell were imputed into CellChat to determine the potential ligand-receptor pairs. Only receptors and ligands whose expression was detected in more than 10 cells were included in this analysis. Pairs with a *P*-value > 0.05 were filtered out from further analysis. The number and weight of intercellular communication in fibroblasts and total cells were compared between Ctrl and TR groups, as well as the cellular communication among AV, CAVD, Ctrl, and TR groups. The "rankNet" function was used to calculate the comparison of pathway information flow based on the Wilcoxon test. The "identifyOverExpressedGenes" function was used to identify overexpressed signaling genes associated with each cell group. Upregulation was defined as $\log_2$-transformed expression > 0.2 for ligand genes, while downregulation was defined as $\log_2$-transformed expression < −0.1 for ligand genes and <−0.1 for receptor genes.

4.6. Transcription Factor Activity Analysis

The SCENIC (v1.3.1) package was used for transcription factor activity analysis. The co-expression modules were based on cisTarget databases (hg38_refseq-r80_10kb_up_and_down_tss, hg38_refseq-r80_500bp_up_and_100bp_down_tss). A total of 6832 fibroblasts and myofibroblasts (10% of the total 68320 fibroblasts and myofibroblasts) were randomly selected and used as input at the network inference step. The AUCell scores were then calculated using all 68320 fibroblasts and myofibroblasts. For other cell types, all cells were used as input at the network inference step and to calculate AUCell scores.

4.7. Protein-Protein Interaction Network

The STRING analysis (v12.0) was applied to study protein-protein-interaction (PPI) between DEGs. Initially, we identified the top 50 DEGs in fibroblasts, endothelial cells, and macrophages using the "FindMarkers" function mentioned earlier. These DEGs were up-regulated or down-regulated in the TR group compared to the Ctrl group. The STRING analysis provided high-confidence PPI interactions based on the neighborhood, gene fusion, co-occurrence, co-expression, experiments, text-mining, and so on. In this study, only interactions for homo sapiens were considered, and a confidence score > 0.4 was requested.

4.8. Pseudo-Time Analysis

Monocle2 (v2.28.0) was used for constructing pseudo-time trajectories. Fifty thousand cells from fibroblasts were selected according to the proportion of each cluster for pseudotime trajectory construction. The cell information was extracted, and an R object was constructed using the "newCellDataSet" function with lowerDetectionLimit = 0.5 and the expressionFamily parameter set as "negbinomial.size ()". Then, the size factor and dispersion were estimated using the "estimateSizeFactors" and "estimateDispersions" functions, and low-quality cells with an average expression level > 0.1 and genes expressed in at least 10 cells were filtered out. The top 400 genes were selected as sorting genes based on q-value using the dpFeature method. Finally, the dimensionality reduction and construction of the pseudo-time trajectories were completed.

4.9. Statistical Analysis

R (version 4.3.1) was used for the statistical analysis. The Wilcoxon Rank Sum test by the Seurat (version 4.4.0) FindAllMarkers function was used to identify differentially expressed genes (DEGs) between the cell clusters. The cell ratios of each type were compared using the Wilcoxon rank sum test. A *P*-value of <0.05 was considered statistically significant.

4.10. Data Accessibility

The TR scRNA-seq datasets were downloaded from the Genome Sequence Archive (Genomics, Proteomics & Bioinformatics 2021) in the National Genomics Data Center, China National Center for Bioinformation/Beijing Institute of Genomics, Chinese Academy of Sciences, under accession code HRA010091 at https://ngdc.cncb.ac.cn/gsa-human. The CAVD scRNA-seq datasets were downloaded from PRJNA562645 at https://ncbi.nlm.nih.gov/bioproject. A total of 16 samples were included (TR: n = 5, control: n = 5; CAVD: n = 4, control: n = 2). Datasets were processed separately and integrated using Harmony to correct for batch effects across samples while preserving biological differences. All analyses were performed using R (v4.3.1). The processed single-cell RNA sequencing data, including expression matrices, cell annotations, and metadata, have been deposited in the Zenodo repository and are publicly available at https://doi.org/10.5281/zenodo.19568228. Patient information is recorded in Supplementary Table. The aortic valve data were obtained from a public dataset comprising 6 individuals (2 healthy controls and 4 CAVD patients), and healthy control aortic valve tissues were harvested from patients undergoing aortic valve replacement during repair of aortic dissection. The tricuspid valve data were obtained from another public dataset comprising 10 individuals (5 controls and 5 with moderate-to-severe functional regurgitation), and control tricuspid valves were collected from transplanted hearts with normal tricuspid structure and function.

Authors' Contributions

Q.G. and J.W. designed and performed research. Q.G., J.W., and M.W. analyzed data and wrote the paper. J.W. and M.W. contributed equally. R.J. and D.X. performed the research and helped with the analysis. X.W. and J.H. managed the project and provided resources. All the authors reviewed the manuscript.

Funding

This work was supported by grants from the National Natural Science Foundation of China (32571042, 32270935, Q.G.), Beijing Natural Science Foundation (7242087, Q.G.), and the Non-Profit Central Research Institute Fund of Chinese Academy of Medical Sciences (2018PT31039).

Conflicts of Interest

The authors declare no conflicts of interest regarding the publication of this paper.

References

[1] Singh, J.P., Evans, J.C., Levy, D., Larson, M.G., Freed, L.A., Fuller, D.L., *et al.* (1999) Prevalence and Clinical Determinants of Mitral, Tricuspid, and Aortic Regurgitation (the Framingham Heart Study). *The American Journal of Cardiology*, **83**, 897-902. https://doi.org/10.1016/s0002-9149(98)01064-9

[2] Samim, D., Dernektsi, C., Brugger, N., Reineke, D. and Praz, F. (2023) Contemporary Approach to Tricuspid Regurgitation: Knowns, Unknowns, and Future Challenges. *Canadian Journal of Cardiology*, **40**, 185-200. https://doi.org/10.1016/j.cjca.2023.11.041

[3] Hahn, R.T., Badano, L.P., Bartko, P.E., Muraru, D., Maisano, F., Zamorano, J.L., *et al.* (2022) Tricuspid Regurgitation: Recent Advances in Understanding Pathophysiology, Severity Grading and Outcome. *European Heart Journal—Cardiovascular Imaging*, **23**, 913-929. https://doi.org/10.1093/ehjci/jeac009

[4] Vahanian, A., Praz, F., Milojevic, M. and Beyersdorf, F. (2021) The "Ten Commandments" for the 2021 ESC/EACTS Guidelines on Valvular Heart Disease. *European Heart Journal*, **42**, 4207-4208. https://doi.org/10.1093/eurheartj/ehab626

[5] Salerno, N., Panuccio, G., Sabatino, J., Leo, I., Torella, M., Sorrentino, S., *et al.* (2023) Cellular and Molecular Mechanisms Underlying Tricuspid Valve Development and Disease. *Journal of Clinical Medicine*, **12**, Article No. 3454. https://doi.org/10.3390/jcm12103454

[6] Nakamura, M. and Sadoshima, J. (2018) Mechanisms of Physiological and Pathological Cardiac Hypertrophy. *Nature Reviews Cardiology*, **15**, 387-407. https://doi.org/10.1038/s41569-018-0007-y

[7] Pitoulis, F.G. and Terracciano, C.M. (2020) Heart Plasticity in Response to Pressure- and Volume-Overload: A Review of Findings in Compensated and Decompensated Phenotypes. *Frontiers in Physiology*, **11**, Article No. 92. https://doi.org/10.3389/fphys.2020.00092

[8] Tian, C., Yang, Y., Ke, Y., Yang, L., Zhong, L., Wang, Z., *et al.* (2021) Integrative Analyses of Genes Associated with Right Ventricular Cardiomyopathy Induced by Tricuspid Regurgitation. *Frontiers in Genetics*, **12**, Article ID: 708275. https://doi.org/10.3389/fgene.2021.708275

[9] Havlenova, T., Skaroupkova, P., Miklovic, M., Behounek, M., Chmel, M., Jarkovska, D., *et al.* (2021) Right versus Left Ventricular Remodeling in Heart Failure Due to Chronic Volume Overload. *Scientific Reports*, **11**, Article No. 17136. https://doi.org/10.1038/s41598-021-96618-8

[10] Moncla, L.M., Briend, M., Bossé, Y. and Mathieu, P. (2023) Calcific Aortic Valve Disease: Mechanisms, Prevention and Treatment. *Nature Reviews Cardiology*, **20**, 546-559. https://doi.org/10.1038/s41569-023-00845-7

[11] Decano, J.L., Iwamoto, Y., Goto, S., Lee, J.Y., Matamalas, J.T., Halu, A., *et al.* (2022) A Disease-Driver Population within Interstitial Cells of Human Calcific Aortic Valves Identified via Single-Cell and Proteomic Profiling. *Cell Reports*, **39**, Article ID: 110685. https://doi.org/10.1016/j.celrep.2022.110685

[12] Shu, S., Fu, M., Chen, X., Zhang, N., Zhao, R., Chang, Y., *et al.* (2022) Cellular Landscapes of Nondiseased Human Cardiac Valves from End-Stage Heart Failure-Explanted Heart. *Arteriosclerosis, Thrombosis, and Vascular Biology*, **42**, 1429-1446. https://doi.org/10.1161/atvbaha.122.318314

[13] Xu, K., Xie, S., Huang, Y., Zhou, T., Liu, M., Zhu, P., *et al.* (2020) Cell-Type Transcriptome Atlas of Human Aortic Valves Reveal Cell Heterogeneity and Endothelial to Mesenchymal Transition Involved in Calcific Aortic Valve Disease. *Arteriosclerosis, Thrombosis, and Vascular Biology*, **40**, 2910-2921. https://doi.org/10.1161/atvbaha.120.314789

[14] Aaltonen, J., Björses, P., Perheentupa, J., Horelli-Kuitunen, N., Palotie, A., Peltonen, L., *et al.* (1997) An Autoimmune Disease, APECED, Caused by Mutations in a Novel Gene Featuring Two PHD-Type Zinc-Finger Domains. *Nature Genetics*, **17**, 399-403. https://doi.org/10.1038/ng1297-399

[15] Jin, Q.H., Kim, H.K., Na, J.Y., Jin, C. and Seon, J.K. (2022) Anti-Inflammatory Effects of Mesenchymal Stem Cell-Conditioned Media Inhibited Macrophages Activation *in Vitro*. *Scientific Reports*, **12**, Article No. 4754. https://doi.org/10.1038/s41598-022-08398-4

[16] Litviňuková, M., Talavera-López, C., Maatz, H., Reichart, D., Worth, C.L., Lindberg, E.L., *et al.* (2020) Cells of the Adult Human Heart. *Nature*, **588**, 466-472. https://doi.org/10.1038/s41586-020-2797-4

[17] Vallecillo-García, P., Orgeur, M., vom Hofe-Schneider, S., Stumm, J., Kappert, V., Ibrahim, D.M., *et al.* (2017) Odd Skipped-Related 1 Identifies a Population of Embryonic Fibro-Adipogenic Progenitors Regulating Myogenesis during Limb Development. *Nature Communications*, **8**, Article No. 1218. https://doi.org/10.1038/s41467-017-01120-3

[18] Lis, G.J., Dubrowski, A., Lis, M., Solewski, B., Witkowska, K., Aleksandrovych, V., *et al.* (2020) Identification of CD34+/PGDFRα+ Valve Interstitial Cells (VICs) in Human Aortic Valves: Association of Their Abundance, Morphology and Spatial Organization with Early Calcific Remodeling. *International Journal of Molecular Sciences*, **21**, Article No. 6330. https://doi.org/10.3390/ijms21176330

[19] Dittrich, G.M., Froese, N., Wang, X., Kroeger, H., Wang, H., Szaroszyk, M., *et al.* (2021) Fibroblast GATA-4 and GATA-6 Promote Myocardial Adaptation to Pressure Overload by Enhancing Cardiac Angiogenesis. *Basic Research in Cardiology*, **116**, Article No. 26. https://doi.org/10.1007/s00395-021-00862-y

[20] Wang, B., Tan, Y., Zhang, Y., Zhang, S., Duan, X., Jiang, Y., *et al.* (2022) Loss of KDM5B Ameliorates Pathological Cardiac Fibrosis and Dysfunction by Epigenetically Enhancing ATF3 Expression. *Experimental & Molecular Medicine*, **54**, 2175-2187. https://doi.org/10.1038/s12276-022-00904-y

[21] Alexanian, M., Przytycki, P.F., Micheletti, R., Padmanabhan, A., Ye, L., Travers, J.G.,

et al. (2021) A Transcriptional Switch Governs Fibroblast Activation in Heart Disease. *Nature*, **595**, 438-443. https://doi.org/10.1038/s41586-021-03674-1

[22] Oka, T., Xu, J., Kaiser, R.A., Melendez, J., Hambleton, M., Sargent, M.A., *et al.* (2007) Genetic Manipulation of Periostin Expression Reveals a Role in Cardiac Hypertrophy and Ventricular Remodeling. *Circulation Research*, **101**, 313-321. https://doi.org/10.1161/circresaha.107.149047

[23] Bermingham, J.R., Shearin, H., Pennington, J., O'Moore, J., Jaegle, M., Driegen, S., *et al.* (2006) The Claw Paw Mutation Reveals a Role for Lgi4 in Peripheral Nerve Development. *Nature Neuroscience*, **9**, 76-84. https://doi.org/10.1038/nn1598

[24] Sanchez-Roige, S., Barnes, S.A., Mallari, J., Wood, R., Polesskaya, O. and Palmer, A.A. (2022) A Mutant Allele of Glycoprotein M6-B (*Gpm6b*) Facilitates Behavioral Flexibility but Increases Delay Discounting. *Genes, Brain and Behavior*, **21**, e12800. https://doi.org/10.1111/gbb.12800

[25] Kim, J., Han, D., Byun, S., Kwon, M., Cho, J.Y., Pleasure, S.J., *et al.* (2018) Ttyh1 Regulates Embryonic Neural Stem Cell Properties by Enhancing the Notch Signaling Pathway. *EMBO Reports*, **19**, EMBR201745472. https://doi.org/10.15252/embr.201745472

[26] Chen, Y., Zhao, X., Sun, J., Su, W., Zhang, L., Li, Y., *et al.* (2019) YAP1/Twist Promotes Fibroblast Activation and Lung Fibrosis That Conferred by miR-15a Loss in Ipf. *Cell Death & Differentiation*, **26**, 1832-1844. https://doi.org/10.1038/s41418-018-0250-0

[27] Gomes, R.N., Manuel, F. and Nascimento, D.S. (2021) The Bright Side of Fibroblasts: Molecular Signature and Regenerative Cues in Major Organs. *NPJ Regenerative Medicine*, **6**, Article No. 43. https://doi.org/10.1038/s41536-021-00153-z

[28] Scharf, G.M., Kilian, K., Cordero, J., Wang, Y., Grund, A., Hofmann, M., *et al.* (2019) Inactivation of Sox9 in Fibroblasts Reduces Cardiac Fibrosis and Inflammation. *JCI Insight*, **4**, e126721. https://doi.org/10.1172/jci.insight.126721

[29] Wu, M., Skaug, B., Bi, X., Mills, T., Salazar, G., Zhou, X., *et al.* (2019) Interferon Regulatory Factor 7 (IRF7) Represents a Link between Inflammation and Fibrosis in the Pathogenesis of Systemic Sclerosis. *Annals of the Rheumatic Diseases*, **78**, 1583-1591. https://doi.org/10.1136/annrheumdis-2019-215208

[30] Liu, Z.Y., Liu, Y., Yu, Z.Y., *et al.* (2024) APOE-NOTCH Axis Governs Elastogenesis during Human Cardiac Valve Remodeling. *Nature Cardiovascular Research*, **3**, 933-950.

[31] Krężel, A. and Maret, W. (2021) The Bioinorganic Chemistry of Mammalian Metallothioneins. *Chemical Reviews*, **121**, 14594-14648. https://doi.org/10.1021/acs.chemrev.1c00371

[32] Rosenzweig, R., Nillegoda, N.B., Mayer, M.P. and Bukau, B. (2019) The Hsp70 Chaperone Network. *Nature Reviews Molecular Cell Biology*, **20**, 665-680. https://doi.org/10.1038/s41580-019-0133-3

[33] Chiosis, G., Digwal, C.S., Trepel, J.B. and Neckers, L. (2023) Structural and Functional Complexity of HSP90 in Cellular Homeostasis and Disease. *Nature Reviews Molecular Cell Biology*, **24**, 797-815. https://doi.org/10.1038/s41580-023-00640-9

[34] Filippou, P.S., Karagiannis, G.S. and Constantinidou, A. (2020) Midkine (MDK) Growth Factor: A Key Player in Cancer Progression and a Promising Therapeutic Target. *Oncogene*, **39**, 2040-2054. https://doi.org/10.1038/s41388-019-1124-8

[35] Tang, Y., Lin, X., Chen, C., Tong, Z., Sun, H., Li, Y., *et al.* (2021) Nucleolin Improves Heart Function during Recovery from Myocardial Infarction by Modulating Macro-

phage Polarization. *Journal of Cardiovascular Pharmacology and Therapeutics*, **26**, 386-395. https://doi.org/10.1177/1074248421989570

[36] Jia, Y., Yu, Y. and Li, H. (2021) POSTN Promotes Proliferation and Epithelial-Mesenchymal Transition in Renal Cell Carcinoma through ILK/AKT/mTOR Pathway. *Journal of Cancer*, **12**, 4183-4195. https://doi.org/10.7150/jca.51253

[37] Xu, C., Zhu, S., Wu, M., Han, W. and Yu, Y. (2014) Functional Receptors and Intracellular Signal Pathways of Midkine (MK) and Pleiotrophin (PTN). *Biological and Pharmaceutical Bulletin*, **37**, 511-520. https://doi.org/10.1248/bpb.b13-00845

[38] Zhou, Q., Cao, H., Hang, X., Liang, H., Zhu, M., Fan, Y., *et al.* (2021) Midkine Prevents Calcification of Aortic Valve Interstitial Cells via Intercellular Crosstalk. *Frontiers in Cell and Developmental Biology*, **9**, Article ID: 794058. https://doi.org/10.3389/fcell.2021.794058

[39] Li, J., Wei, H., Chesley, A., Moon, C., Krawczyk, M., Volkova, M., *et al.* (2007) The Pro-Angiogenic Cytokine Pleiotrophin Potentiates Cardiomyocyte Apoptosis through Inhibition of Endogenous AKT/PKB Activity. *Journal of Biological Chemistry*, **282**, 34984-34993. https://doi.org/10.1074/jbc.m703513200

[40] Majaj, M. and Weckbach, L.T. (2022) Midkine—A Novel Player in Cardiovascular Diseases. *Frontiers in Cardiovascular Medicine*, **9**, Article ID: 1003104. https://doi.org/10.3389/fcvm.2022.1003104

[41] Thorin, E., Labbé, P., Lambert, M., Mury, P., Dagher, O., Miquel, G., *et al.* (2023) Angiopoietin-Like Proteins: Cardiovascular Biology and Therapeutic Targeting for the Prevention of Cardiovascular Diseases. *Canadian Journal of Cardiology*, **39**, 1736-1756. https://doi.org/10.1016/j.cjca.2023.06.002

[42] Cho, D.I., Ahn, M.J., Cho, H.H., Cho, M., Jun, J.H., Kang, B.G., *et al.* (2023) ANGPTL4 Stabilizes Atherosclerotic Plaques and Modulates the Phenotypic Transition of Vascular Smooth Muscle Cells through KLF4 Downregulation. *Experimental & Molecular Medicine*, **55**, 426-442. https://doi.org/10.1038/s12276-023-00937-x

[43] Andrews, J.P., Marttala, J., Macarak, E., Rosenbloom, J. and Uitto, J. (2016) Keloids: The Paradigm of Skin Fibrosis—Pathomechanisms and Treatment. *Matrix Biology*, **51**, 37-46. https://doi.org/10.1016/j.matbio.2016.01.013

[44] Murota, H., Lingli, Y. and Katayama, I. (2017) Periostin in the Pathogenesis of Skin Diseases. *Cellular and Molecular Life Sciences*, **74**, 4321-4328. https://doi.org/10.1007/s00018-017-2647-1

[45] O'Dwyer, D.N. and Moore, B.B. (2017) The Role of Periostin in Lung Fibrosis and Airway Remodeling. *Cellular and Molecular Life Sciences*, **74**, 4305-4314. https://doi.org/10.1007/s00018-017-2649-z

[46] Tan, C., Ge, Z., Kurup, S., Dyakiv, Y., Liu, T., Muller, W.A., *et al.* (2024) FOXC1 and FOXC2 Ablation Causes Abnormal Valvular Endothelial Cell Junctions and Lymphatic Vessel Formation in Myxomatous Mitral Valve Degeneration. *Arteriosclerosis, Thrombosis, and Vascular Biology*, **44**, 1944-1959. https://doi.org/10.1161/atvbaha.124.320316

[47] Chang, C., Neilson, J.R., Bayle, J.H., Gestwicki, J.E., Kuo, A., Stankunas, K., *et al.* (2004) A Field of Myocardial-Endocardial NFAT Signaling Underlies Heart Valve Morphogenesis. *Cell*, **118**, 649-663. https://doi.org/10.1016/j.cell.2004.08.010

[48] Almalki, W.H. (2024) Unraveling the Role of Xist RNA in Cardiovascular Pathogenesis. *Pathology—Research and Practice*, **253**, Article ID: 154944. https://doi.org/10.1016/j.prp.2023.154944

[49] Gerke, V., Gavins, F.N.E., Geisow, M., Grewal, T., Jaiswal, J.K., Nylandsted, J., *et al.* (2024) Annexins—A Family of Proteins with Distinctive Tastes for Cell Signaling and

Membrane Dynamics. *Nature Communications*, **15**, Article No. 1574. https://doi.org/10.1038/s41467-024-45954-0

[50] Liu, M., Zhang, L., Marsboom, G., Jambusaria, A., Xiong, S., Toth, P.T., *et al.* (2019) Sox17 Is Required for Endothelial Regeneration Following Inflammation-Induced Vascular Injury. *Nature Communications*, **10**, Article No. 2126. https://doi.org/10.1038/s41467-019-10134-y

[51] Tsaryk, R., Yucel, N., Leonard, E.V., Diaz, N., Bondareva, O., Odenthal-Schnittler, M., *et al.* (2022) Shear Stress Switches the Association of Endothelial Enhancers from ETV/ETS to KLF Transcription Factor Binding Sites. *Scientific Reports*, **12**, Article No. 4795. https://doi.org/10.1038/s41598-022-08645-8

[52] Zhu, X., Zhang, X.G., Gu, W., *et al.* (2023) ANGPTL4 Suppresses the Profibrogenic Functions of Atrial Fibroblasts Induced by Angiotensin II by Up-Regulating PPAR*γ*. *Iranian Journal of Basic Medical Sciences*, **26**, 587-593.

[53] Sierro, F., Biben, C., Martínez-Muñoz, L., Mellado, M., Ransohoff, R.M., Li, M., *et al.* (2007) Disrupted Cardiac Development but Normal Hematopoiesis in Mice Deficient in the Second CXCL12/SDF-1 Receptor, CXCR7. *Proceedings of the National Academy of Sciences*, **104**, 14759-14764. https://doi.org/10.1073/pnas.0702229104

[54] Dogra, D., Ahuja, S., Kim, H., Rasouli, S.J., Stainier, D.Y.R. and Reischauer, S. (2017) Opposite Effects of Activin Type 2 Receptor Ligands on Cardiomyocyte Proliferation during Development and Repair. *Nature Communications*, **8**, Article No. 1902. https://doi.org/10.1038/s41467-017-01950-1

[55] Nibbs, R.J.B. and Graham, G.J. (2013) Immune Regulation by Atypical Chemokine Receptors. *Nature Reviews Immunology*, **13**, 815-829. https://doi.org/10.1038/nri3544

[56] Ensan, S., Li, A., Besla, R., Degousee, N., Cosme, J., Roufaiel, M., *et al.* (2016) Self-renewing Resident Arterial Macrophages Arise from Embryonic CX3CR1+ Precursors and Circulating Monocytes Immediately after Birth. *Nature Immunology*, **17**, 159-168. https://doi.org/10.1038/ni.3343

[57] Vanneste, D., Bai, Q., Hasan, S., Peng, W., Pirottin, D., Schyns, J., *et al.* (2023) Mafb-restricted Local Monocyte Proliferation Precedes Lung Interstitial Macrophage Differentiation. *Nature Immunology*, **24**, 827-840. https://doi.org/10.1038/s41590-023-01468-3

[58] Zhou, S., Zhao, T., Chen, X., Zhang, W., Zou, X., Yang, Y., *et al.* (2023) Runx1 Deficiency Promotes M2 Macrophage Polarization through Enhancing STAT6 Phosphorylation. *Inflammation*, **46**, 2241-2253. https://doi.org/10.1007/s10753-023-01874-7

[59] Dick, S.A., Macklin, J.A., Nejat, S., Momen, A., Clemente-Casares, X., Althagafi, M.G., *et al.* (2018) Self-Renewing Resident Cardiac Macrophages Limit Adverse Remodeling Following Myocardial Infarction. *Nature Immunology*, **20**, 29-39. https://doi.org/10.1038/s41590-018-0272-2

[60] Xia, C., Braunstein, Z., Toomey, A.C., Zhong, J. and Rao, X. (2018) S100 Proteins as an Important Regulator of Macrophage Inflammation. *Frontiers in Immunology*, **8**, Article No. 1908. https://doi.org/10.3389/fimmu.2017.01908

[61] Dulyaninova, N.G., Ruiz, P.D., Gamble, M.J., Backer, J.M. and Bresnick, A.R. (2018) S100A4 Regulates Macrophage Invasion by Distinct Myosin-Dependent and Myosin-Independent Mechanisms. *Molecular Biology of the Cell*, **29**, 632-642. https://doi.org/10.1091/mbc.e17-07-0460

[62] Kobori, T., Hamasaki, S., Kitaura, A., Yamazaki, Y., Nishinaka, T., Niwa, A., *et al.* (2018) Interleukin-18 Amplifies Macrophage Polarization and Morphological Alteration, Leading to Excessive Angiogenesis. *Frontiers in Immunology*, **9**, Article No.

334. https://doi.org/10.3389/fimmu.2018.00334

[63] Zhang, L., Ran, L., Garcia, G.E., Wang, X.H., Han, S., Du, J., *et al.* (2009) Chemokine CXCL16 Regulates Neutrophil and Macrophage Infiltration into Injured Muscle, Promoting Muscle Regeneration. *The American Journal of Pathology*, **175**, 2518-2527. https://doi.org/10.2353/ajpath.2009.090275

[64] Wu, Q., Sun, S., Wei, L., Liu, M., Liu, H., Liu, T., *et al.* (2022) Twist1 Regulates Macrophage Plasticity to Promote Renal Fibrosis through Galectin-3. *Cellular and Molecular Life Sciences*, **79**, Article No. 137. https://doi.org/10.1007/s00018-022-04137-0

[65] Chakraborty, S., Wirrig, E.E., Hinton, R.B., Merrill, W.H., Spicer, D.B. and Yutzey, K.E. (2010) Twist1 Promotes Heart Valve Cell Proliferation and Extracellular Matrix Gene Expression during Development *in Vivo* and Is Expressed in Human Diseased Aortic Valves. *Developmental Biology*, **347**, 167-179. https://doi.org/10.1016/j.ydbio.2010.08.021

[66] Kuppe, C., Ramirez Flores, R.O., Li, Z., Hayat, S., Levinson, R.T., Liao, X., *et al.* (2022) Spatial Multi-Omic Map of Human Myocardial Infarction. *Nature*, **608**, 766-777. https://doi.org/10.1038/s41586-022-05060-x

[67] Han, P., Che, X., Li, H., Gao, Y., Wei, X. and Li, P. (2020) Annexin A1 Involved in the Regulation of Inflammation and Cell Signaling Pathways. *Chinese Journal of Traumatology*, **23**, 96-101. https://doi.org/10.1016/j.cjtee.2020.02.002

[68] Varricchi, G., Marone, G. and Kovanen, P.T. (2020) Cardiac Mast Cells: Underappreciated Immune Cells in Cardiovascular Homeostasis and Disease. *Trends in Immunology*, **41**, 734-746. https://doi.org/10.1016/j.it.2020.06.006

[69] Hahn, R.T. (2023) Tricuspid Regurgitation. *New England Journal of Medicine*, **388**, 1876-1891. https://doi.org/10.1056/nejmra2216709

[70] Asmarats, L., Taramasso, M. and Rodés-Cabau, J. (2019) Tricuspid Valve Disease: Diagnosis, Prognosis and Management of a Rapidly Evolving Field. *Nature Reviews Cardiology*, **16**, 538-554. https://doi.org/10.1038/s41569-019-0186-1

[71] Rutkovskiy, A., Malashicheva, A., Sullivan, G., Bogdanova, M., Kostareva, A., Stensløkken, K., *et al.* (2017) Valve Interstitial Cells: The Key to Understanding the Pathophysiology of Heart Valve Calcification. *Journal of the American Heart Association*, **6**, e006339. https://doi.org/10.1161/jaha.117.006339

[72] Bian, W., Wang, Z., Sun, C. and Zhang, D.M. (2021) Pathogenesis and Molecular Immune Mechanism of Calcified Aortic Valve Disease. *Frontiers in Cardiovascular Medicine*, **8**, Article 765419. https://doi.org/10.3389/fcvm.2021.765419

[73] Ren, H., Walker, B.L., Cang, Z. and Nie, Q. (2022) Identifying Multicellular Spatiotemporal Organization of Cells with SpaceFlow. *Nature Communications*, **13**, Article No. 4076. https://doi.org/10.1038/s41467-022-31739-w

[74] Hashimoto, M., Kojima, Y., Sakamoto, T., Ozato, Y., Nakano, Y., Abe, T., *et al.* (2024) Spatial and Single-Cell Colocalisation Analysis Reveals Mdk-Mediated Immunosuppressive Environment with Regulatory T Cells in Colorectal Carcinogenesis. *eBioMedicine*, **103**, Article ID: 105102. https://doi.org/10.1016/j.ebiom.2024.105102

[75] Dai, X., Tan, Y., Cai, S., Xiong, X., Wang, L., Ye, Q., *et al.* (2011) The Role of CXCR7 on the Adhesion, Proliferation and Angiogenesis of Endothelial Progenitor Cells. *Journal of Cellular and Molecular Medicine*, **15**, 1299-1309. https://doi.org/10.1111/j.1582-4934.2011.01301.x

[76] Rajagopal, S., Kim, J., Ahn, S., Craig, S., Lam, C.M., Gerard, N.P., *et al.* (2009) β-Arrestin—But Not G Protein-Mediated Signaling by the "Decoy" Receptor CXCR7. *Proceedings of the National Academy of Sciences*, **107**, 628-632.

https://doi.org/10.1073/pnas.0912852107

[77] Duval, V., Alayrac, P., Silvestre, J. and Levoye, A. (2022) Emerging Roles of the Atypical Chemokine Receptor 3 (ACKR3) in Cardiovascular Diseases. *Frontiers in Endocrinology*, **13**, Article ID: 906586. https://doi.org/10.3389/fendo.2022.906586

[78] Ishizuka, M., Harada, M., Nomura, S., Ko, T., Ikeda, Y., Guo, J., *et al.* (2021) CXCR7 Ameliorates Myocardial Infarction as a *β*-Arrestin-Biased Receptor. *Scientific Reports*, **11**, Article No. 3426. https://doi.org/10.1038/s41598-021-83022-5

[79] Yu, S., Crawford, D., Tsuchihashi, T., Behrens, T.W. and Srivastava, D. (2011) The Chemokine Receptor CXCR7 Functions to Regulate Cardiac Valve Remodeling. *Developmental Dynamics*, **240**, 384-393. https://doi.org/10.1002/dvdy.22549

[80] Afzal, A.R., Kiechl, S., Daryani, Y.P., Weerasinghe, A., Zhang, Y., Reindl, M., *et al.* (2008) Common CCR5-del32 Frameshift Mutation Associated with Serum Levels of Inflammatory Markers and Cardiovascular Disease Risk in the Bruneck Population. *Stroke*, **39**, 1972-1978. https://doi.org/10.1161/strokeaha.107.504381

[81] Ortlepp, J., *et al.* (2004) The Amount of Calcium-Deficient Hexagonal Hydroxyapatite in Aortic Valves Is Influenced by Gender and Associated with Genetic Polymorphisms in Patients with Severe Calcific Aortic Stenosis. *European Heart Journal*, **25**, 514-522. https://doi.org/10.1016/j.ehj.2003.09.006

[82] Jones, K., Maguire, J. and Davenport, A. (2011) Chemokine Receptor CCR5: From AIDS to Atherosclerosis. *British Journal of Pharmacology*, **162**, 1453-1469. https://doi.org/10.1111/j.1476-5381.2010.01147.x

[83] Wang, X., Li, W., Yue, Q., Du, W., Li, Y., Liu, F., *et al.* (2020) C-C Chemokine Receptor 5 Signaling Contributes to Cardiac Remodeling and Dysfunction under Pressure Overload. *Molecular Medicine Reports*, **23**, 1. https://doi.org/10.3892/mmr.2020.11687

[84] Mettimano, M., Specchia, M.L., Ianni, A., Arzani, D., Ricciardi, G., Savi, L., *et al.* (2003) CCR5 and CCR2 Gene Polymorphisms in Hypertensive Patients. *British Journal of Biomedical Science*, **60**, 19-21. https://doi.org/10.1080/09674845.2003.11783672

[85] Merryman, W.D., Youn, I., Lukoff, H.D., Krueger, P.M., Guilak, F., Hopkins, R.A., *et al.* (2006) Correlation between Heart Valve Interstitial Cell Stiffness and Transvalvular Pressure: Implications for Collagen Biosynthesis. *American Journal of Physiology-Heart and Circulatory Physiology*, **290**, H224-H231. https://doi.org/10.1152/ajpheart.00521.2005

[86] Merryman, W.D., Liao, J., Parekh, A., Candiello, J.E., Lin, H. and Sacks, M.S. (2007) Differences in Tissue-Remodeling Potential of Aortic and Pulmonary Heart Valve Interstitial Cells. *Tissue Engineering*, **13**, 2281-2289. https://doi.org/10.1089/ten.2006.0324

[87] Peng, Q., Shan, D., Cui, K., Li, K., Zhu, B., Wu, H., *et al.* (2022) The Role of Endothelial-to-Mesenchymal Transition in Cardiovascular Disease. *Cells*, **11**, Article No. 1834. https://doi.org/10.3390/cells11111834

[88] Islam, S., Boström, K.I., Di Carlo, D., Simmons, C.A., Tintut, Y., Yao, Y., *et al.* (2021) The Mechanobiology of Endothelial-to-Mesenchymal Transition in Cardiovascular Disease. *Frontiers in Physiology*, **12**, Article ID: 734215. https://doi.org/10.3389/fphys.2021.734215

[89] Cohen, D.J., Malave, D., Ghidoni, J.J., Iakovidis, P., Everett, M.M., You, S., *et al.* (2004) Role of Oral Bacterial Flora in Calcific Aortic Stenosis: An Animal Model. *The Annals of Thoracic Surgery*, **77**, 537-543. https://doi.org/10.1016/s0003-4975(03)01454-1

[90] Nakano, K., Nemoto, H., Nomura, R., Inaba, H., Yoshioka, H., Taniguchi, K., *et al.* (2009) Detection of Oral Bacteria in Cardiovascular Specimens. *Oral Microbiology and Immunology*, **24**, 64-68. https://doi.org/10.1111/j.1399-302x.2008.00479.x

[91] da Silva, R.M., Lingaas, P.S., Geiran, O., Tronstad, L. and Olsen, I. (2003) Multiple Bacteria in Aortic Aneurysms. *Journal of Vascular Surgery*, **38**, 1384-1389. https://doi.org/10.1016/s0741-5214(03)00926-1

[92] Liu, Z., Li, J., Liu, H., Tang, Y., Zhan, Q., Lai, W., *et al.* (2019) The Intestinal Microbiota Associated with Cardiac Valve Calcification Differs from That of Coronary Artery Disease. *Atherosclerosis*, **284**, 121-128. https://doi.org/10.1016/j.atherosclerosis.2018.11.038

[93] Yoshimatsu, Y. and Watabe, T. (2022) Emerging Roles of Inflammation-Mediated Endothelial-Mesenchymal Transition in Health and Disease. *Inflammation and Regeneration*, **42**, Article No. 9. https://doi.org/10.1186/s41232-021-00186-3

Supplemental Materials

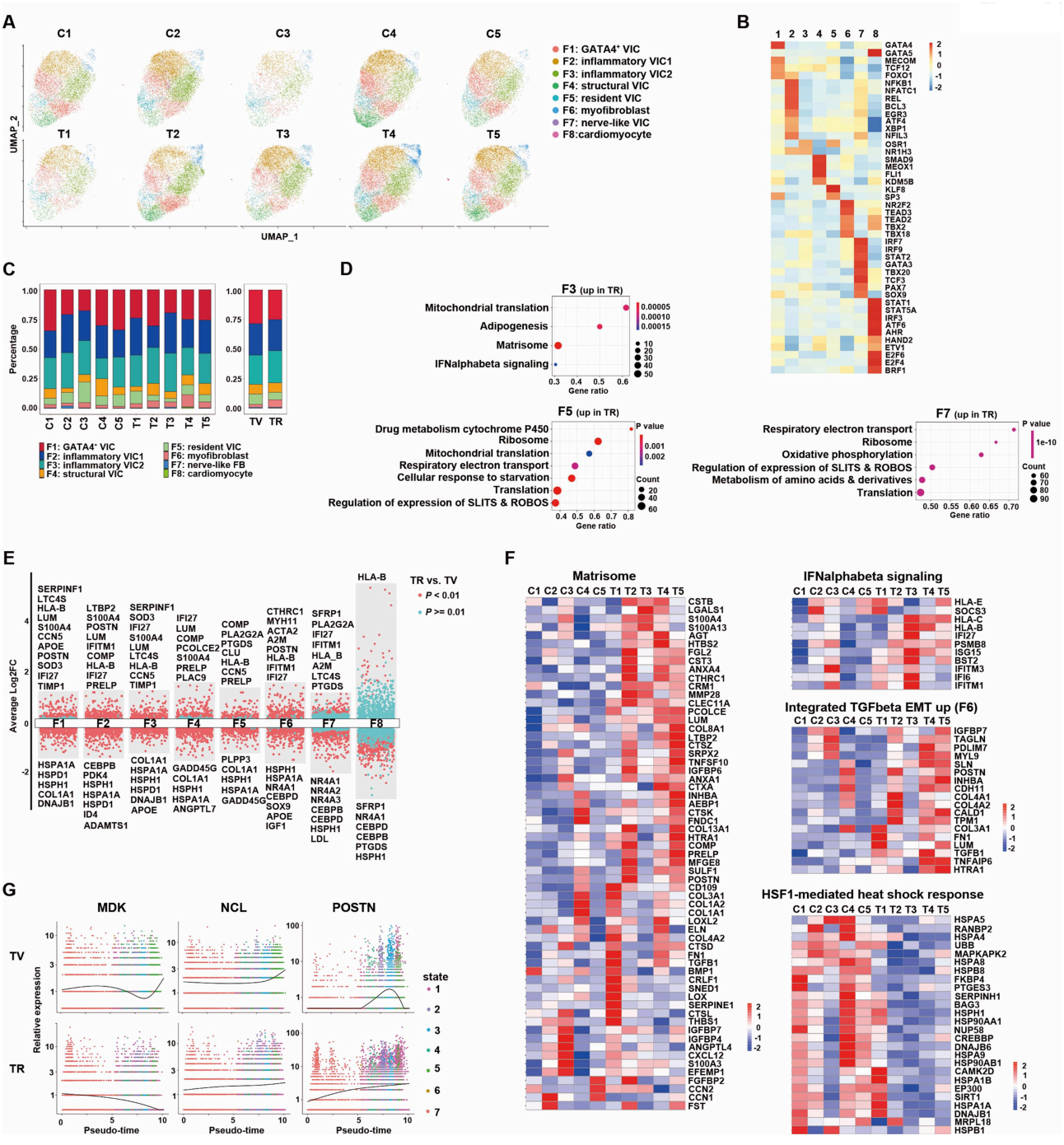

Figure S1. Transcriptome comparison of VICs between TV and TR cohorts.

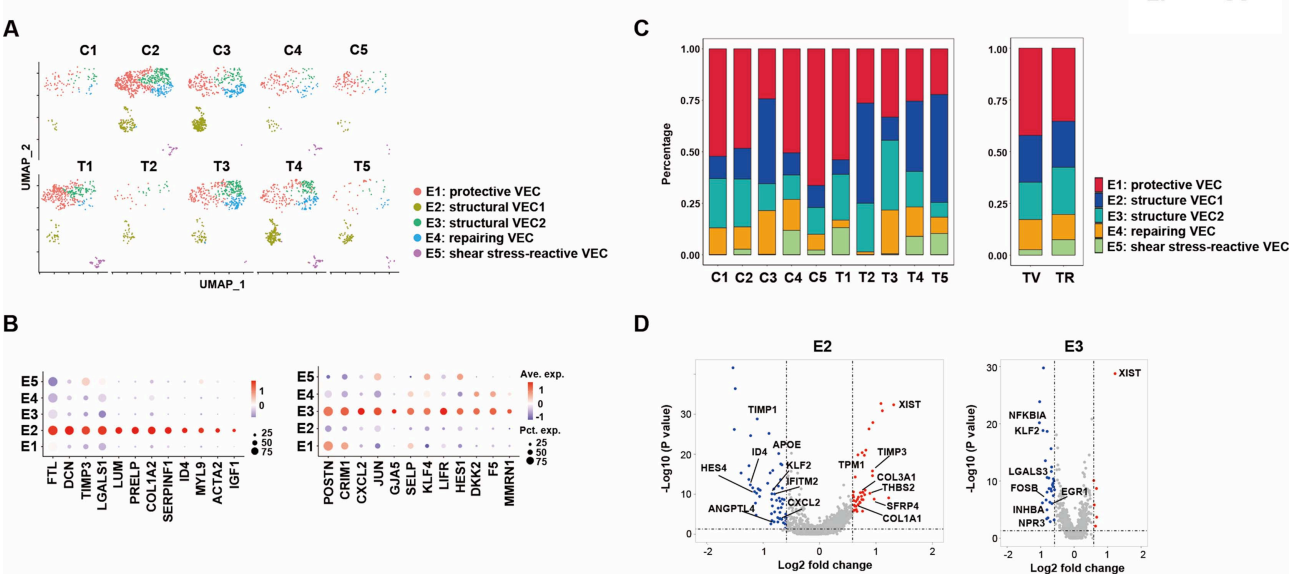

Figure S2. Transcriptome analysis of VECs in TV and TR cohorts.

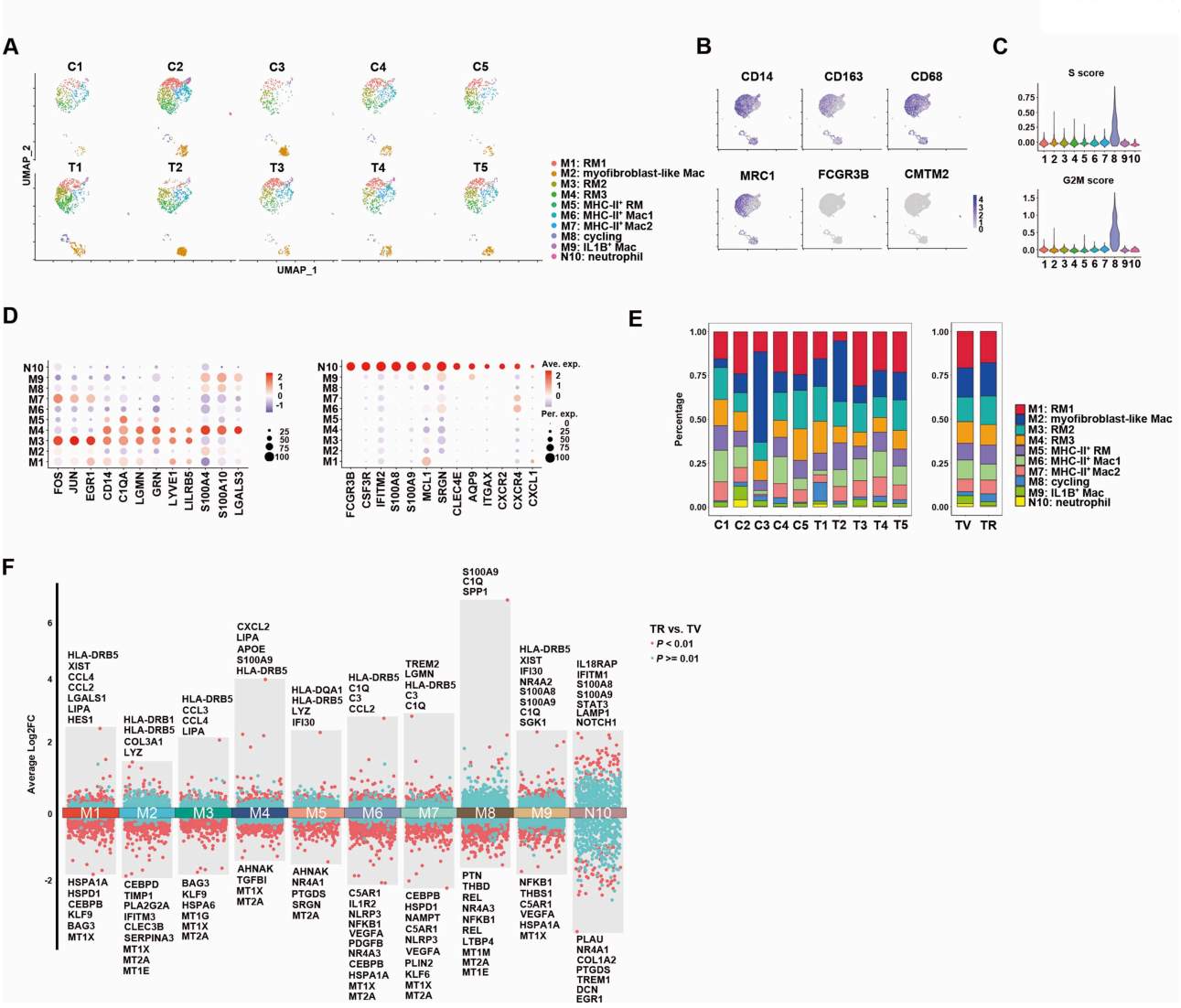

Figure S3. Transcriptome analysis of myeloid cells in TV and TR cohorts.

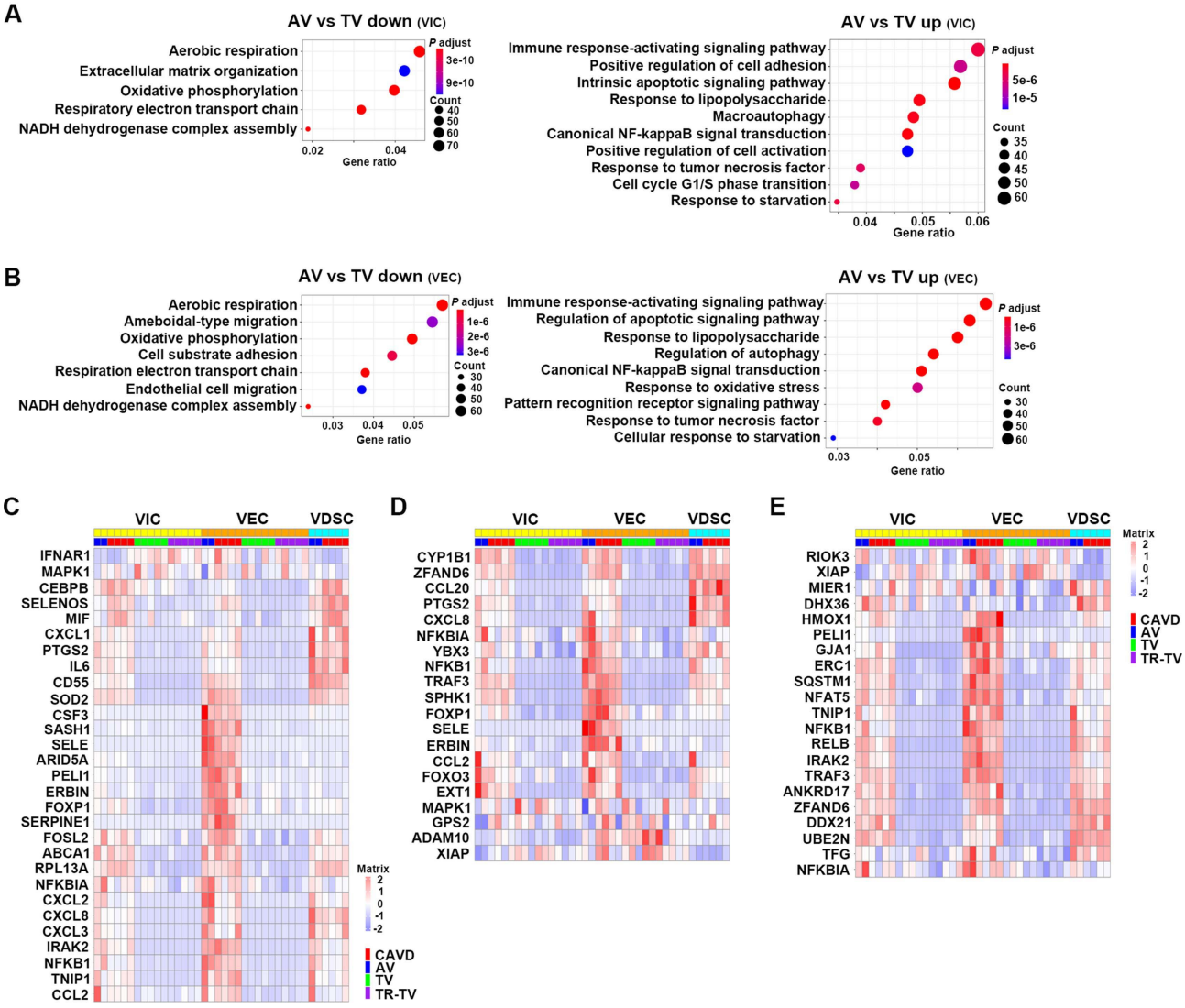

Figure S4. Comparison of the transcriptome and intercellular communications between TV and AV without diseases.

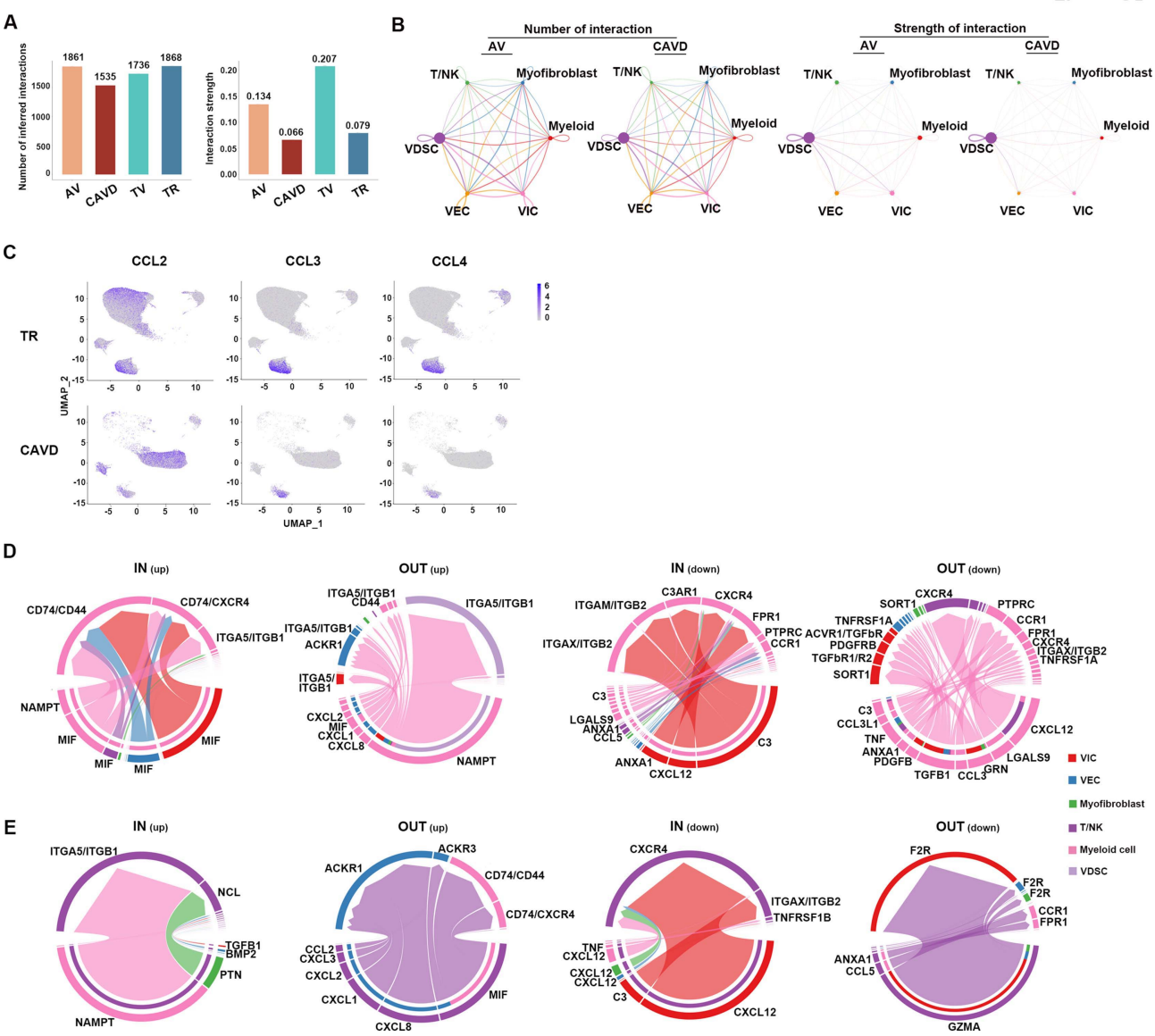

Figure S5. Comparison of the intercellular communications between tricuspid valves obtained from TR and aortic valves obtained from CAVD.

	TV_1	TV_2	TV_3	TV_4	TV_5	TR_1	TR_2	TR_3	TR_4	TR_5	AV_1	AV_2	CAVD_1	CAVD_2	CAVD_3	CAVD_4
Sex	Female	Male	Male	Male	Male	Male	Male	Female	Female	Male	Male	Female	Female	Female	Male	Female
Age, y	16	26	35	11	33	10	55	51	30	36	50	48	52	54	50	56
Tissue Source	TV	TV	TV	TV	TV	TV	TV	TV	TV	TV	AV	AV	AV	AV	AV	AV
BMI, kg/m^2	11.17	24.84	24.65	21.78	21.3	21.1	23.66	30.08	20.81	22.13	NA	NA	NA	NA	NA	NA
Diagnosis	RCM	RCM	DCM	DCM	HCM	DCM	CTGA	DCM	CTGA	CTGA	Aortic Dissection	Aortic Dissection	CAVD	CAVD	CAVD	CAVD
Hyperlipidemia	No	No	No	No	No	No	No	No	No	No	No	No	No	No	No	No
Hypertension	No	No	No	No	No	No	No	No	No	No	No	No	No	No	No	No
Diabetes Mellitus	No	No	No	No	No	No	No	No	No	No	No	No	No	No	No	No
NYHA Class	III	IV	IV	IV	III	IV	III	IV	II-III	III	I	II	III	IV	III	III
LVEF, %	58	62	28	32	31	25	54	28	65	55	60	60	60	56	61	58
Cell Number	8366	12,731	4561	10761	7827	6356	10,414	8898	12,271	12,067	1916	3468	9455	12,025	14,235	5317
Processed Number	7860	12,203	4505	10,062	7432	6116	10,316	8769	11,865	11,788	1686	3198	9026	7259	12,022	4710